Tectonic controls for transverse drainage and timing of the Xin-Ding paleolake breach in the upper reach of the Hutuo River, north China

Citation	Ren, J., Zhang, S., Meigs, A. J., Yeats, R. S., Ding, R., & Shen, X. (2014). Tectonic controls for transverse drainage and timing of the Xin-Ding paleolake breach in the upper reach of the Hutuo River, north China. Geomorphology, 206, 452-467. doi:10.1016/j.geomorph.2013.10.016
DOI	10.1016/j.geomorph.2013.10.016
Publisher	Elsevier
Version	Accepted Manuscript
Terms of Use	http://cdss.library.oregonstate.edu/sa-termsofuse

Tectonic controls for transverse drainage and timing of the Xin-Ding paleolake breach in the upper reach of the Hutuo River, North China

Junjie Ren[1,2,*], Shimin Zhang[1], Andrew J. Meigs[2], Robert S. Yeats[2], Rui Ding[1] and Xiaoming Shen[1]

[1]Key Laboratory of Crustal Dynamics, Institute of Crustal Dynamics, China Earthquake Administration, Beijing 100085, China

[2]College of Earth, Ocean, and Atmospheric Sciences, Oregon State University, Corvallis, OR 97331, USA

*Corresponding author:

Junjie Ren

Institute of Crustal Dynamics

China Earthquake Administration

Xisanqi, Haidian

Beijing 100085, China

Tel.:+86-010-62846730

Fax.: +86-010-62846732

Email: *renjunjie@gmail.com*

Abstract

The upper reach of the Hutuo River flows along the Xin-Ding basin and cuts a transverse drainage through Xizhou Mountain and Taihang Range into the North China Plain. Previous studies showed that the Xin-Ding basin was occupied by a lake during the Early-Middle Pleistocene. However, the timing of the paleolake breach and the mechanism for the creation of the transverse drainage are unknown. We constructed the fluvial terrace sequence in the upper reach of the Hutuo drainage combined with thermoluminescence (TL) and optically stimulated luminescence (OSL) dating, as well as the timescale of the overlying loess-paleosol units. Our results reveal that (1) five terraces (T5-T1) are developed along the upper reach of the Hutuo River, amongst which terraces T4-T1 were formed synchronously at ~600 ka, ~120-130 ka, ~21-26 ka and ~6-7 ka, respectively; (2) the creation of the transverse drainage and breach of the Xin-Ding paleolake occurred between ~600 ka and ~130 ka; (3) the mechanism for the creation of the transverse drainage is via river piracy of paleostreams on both sides of the drainage divide. Localized differential uplift and associated tilting of the Xizhou Mountain block during the Middle Pleistocene result in the formation of the transverse drainage and breach of the Xin-Ding paleolake.

Key words: Transverse drainage; Hutuo River; Xin-Ding paleolake; river piracy; fluvial terrace; loess-paleosol sequence; tectonic uplift

1.Introduction

Drainage reorganization in late Cenozoic has been widely recognized in many of the world's large river systems and extensively studied by geomorphologists (e.g. Blackwelder, 1934; Harvey and Wells, 1987; Bull, 1991; Bishop, 1995; Stokes and Mather, 2003; Clark et al., 2004; Cordier et al., 2006; Stokes, 2008; Stokes et al., 2008; Bridgland et al., 2012). Since at least the 18th century, numerous researchers have noticed the role of transverse drainage and discussed its causes (e.g. Lane, 1899; Twidale, 1966; Hunt, 1971; Lucchitta, 1972). Transverse drainages are streams that cut across tectonically controlled geological structures such as faults, folds and orogenic highlands (Oberlander, 1985; Stokes et al., 2008). They are generally characterized by distinctive but narrow and deeply dissected gorges or canyons that cut through obstructing mountains. In the past decade there is an increasing interest on the mechanism of transverse drainage (Mayer et al., 2003; Stokes and Mather, 2003; Clark et al., 2004; Douglass and Schmeeckle, 2007; Stokes et al., 2008; Douglass et al., 2009).

The creation of transverse drainage can be interpreted by numerous factors (e.g. Twidale, 2004; Stokes et al., 2008; Douglass et al., 2009), but is generally associated with the mechanisms of 1) antecedence (fluvial incision keeps pace with tectonic uplift and growing structures) (e.g. Hasbargen and Paola, 2000; Simpson, 2004), 2) superimposition (a concordant river erosionally removes an overlying sedimentary cover to become discordant with an underlying, differently bedrock/structure) (e.g. Oberlander, 1985; Douglass and Schmeeckle, 2007), 3) overflow (a lake, ponded behind a resistant sill, finally overspills the lower divide because of climate-related lake-level rise) (Meek and Douglass, 2001) and 4) stream piracy (an increasing headward erosion

across an uplifted surface results in the capture and re-routing of a less active stream) (e.g. Harvey and Wells, 1987; Stokes and Mather, 2003). These mechanisms are themselves driven by factors that are internal (e.g. bedrock lithology and geologic structure) or external (climate change, tectonism, and eustacy) to the fluvial system (Stokes and Mather, 2003). Thus, knowledge of the origin of transverse drainage provides insights in the rearrangement of fluvial system and long-term landscape development.

The Hutuo River originates from the northeast of Wutai Mountain, the highest mountain in North China, and flows along the northern part of the Xin-Ding basin, a graben in the northeastern part of the Shanxi rift system (Figs. 1 and 2a). In the southern part of the basin, the river turns eastward to flows along the Dingxiang and Dongye subbasins and cuts a gorge through Xizhou Mountain and Taihang Range into the North China Plain (Fig. 1). The ancestral Hutuo drainage was proposed to flow southward into the Taiyuan basin by the way of the Shilingguan or Taiheling Col and joined the Fenhe River during the Pliocene (Figs. 1 and 2a) (Willis and Blackwelder, 1907; Wang, 1926; Zhang, 1959; Lou and Du, 1960; Li and Liang, 1965; Wang et al., 1996) . Subsequent uplift of the Xizhou Mountain in the Early Pleistocene (Wang et al., 1996) forced the ancestral Hutuo drainage to abandon its southward-flowing channel. Drilling data (Hydrogeological Team of Geological Bureau of Shanxi Province, 1977) revealed that the Xin-Ding basin was dominated by a paleolake during the Early-Middle Pleistocene. However, the timing of the paleolake breach and its mechanism are poorly understood. From the drainage features, the breach of the Xin-Ding paleolake is related to the creation of the transverse drainage where the paleolake links across the Xizhou Mountain to the present Hutuo drainage in the Taihang Range area (hereinafter referred to as the Shihouping-Pingshang transverse drainage) (Fig. 2a). Thus, the mechanism of this

transverse drainage is the key to the paleolake breach.

The drainage incision process may be documented by river terrace development along the ancestral and present valleys (Stokes and Mather, 2003). Thus, in this paper we first map and reconstruct fluvial terrace sequence in the basin and gorge segments of the Hutuo River in combination with field investigations, TL and OSL dating, and the loess-paleosol timescale to determine the timing of the breach of the Xin-Ding paleolake. We then rebuild the long-term drainage evolution of the upper reach of the Hutuo river system. Lastly, we explore the mechanism of the development of the Shihouping-Pingshang transverse drainage and its controlling factors. This study provides a meaningful understanding of the effects of localized differential uplift and related tilting on rivers in a graben setting.

2.Regional setting

The Shanxi rift system is bordered by the Ordos Massif to the west and the Taihang Range to the east and is characterized by an S-shaped string of asymmetric intermontane basins over 1200 km from north to south (Fig. 1) (Xu and Ma, 1992; Zhang et al., 1998). The extension of this rift system was thought to have been driven by large-scale strike-slip faults associated with the collisional interaction of the Indian and Eurasian plates and eastward motion of the Tibetan Plateau (Peltzer et al., 1985; Xu and Ma, 1992; Zhang et al., 1998). This process may have started in the Miocene (Zhang et al., 1998), but the formation of the present grabens occurred mainly since the Pliocene (Xu et al., 1993).

The Xin-Ding graben at the northeastern of the rift system is bounded by Yunzhong Mountain to

the west, Heng Mountain to the north, and Wutai and Xizhou Mountains to the east and south (Fig. 2). This graben is composed of several Neogene subgrabens: Daixian, Yuanping, Dingxiang and Dongye subbasins separated by a series of subhorsts, characterized by several depocenters (Fig. 2b). The mountain fronts are characterized by distinctive fault scarps, numerous stepped landforms and V-shaped valleys. In the uplifted mountain areas, three planation surfaces were identified and regarded as the response of the multistage Tibetan uplift (Li and Fang, 1999). The Tangxian surface is the youngest one that was formed in the Neogene and is widely distributed in North China (Wu et al., 1999). Below the Tangxian surface, at least six alluvial terraces are developed along the mountain-frontal areas, suggestive of episodic uplift during the Quaternary (Zhang et al., 2007). Large mountain-frontal alluvial fans (Ren and Zhang, 2006) and >1800-m-thick late Cenozoic deposits in the graben (Fig. 2b) indicate that the mountains have undergone strong tectonic uplift of the mountains during the late Cenozoic. Displaced alluvial terraces show that the boundary faults of the Xin-Ding basin has an average late-Quaternary vertical slip rate of 1.2-4.2 mm/yr (Xu et al., 1993; Zhang et al., 2007). During historical time, the Xin-Ding basin has experienced three strong earthquakes, the Daixian earthquake (M 7½) in 512 on the Wutai fault, the Dingxiang earthquake (M 7¼) in 1038 on the Xizhou fault, and the Yuanping earthquake (M 7) in 1683 probably on the Yunzhong fault (Fig. 2a) (Xu et al., 1993).

The study area is located in the eastern Chinese Loess Plateau. The Chinese loess-paleosol sequence has been extensively studied (e.g. Liu, 1985; Kukla and An, 1989; Ding et al., 2002) and is divided stratigraphically into successive units, each of which has been assigned a stratigraphic designation (loess units: L_1, L_2, …; paleosol units: S_0, S_1, S_2, …) as described by Sun (2005) (Fig. 3). The loess sections are composed of unweathered massive yellow loess units and red mature

weathered soil units (Liu, 1985; Kukla and An, 1989), which represent the relatively cold and dry, and comparatively wet and mild periods, respectively. This loess-paleosol sequence has been as a paleoclimatic proxy to show that the region of the Loess Plateau has undergone at least 33 glacial-interglacial cycles in the Quaternary (Ding et al., 2002). In addition, the loess-paleosol succession has been well correlated with the standard marine $\delta^{18}O$ series (Fig. 3) (Ding et al., 2002; Ding et al., 2005), hence each loess and paleosol unit can be used as a pronounced regional stratigraphic marker layer of known age(e.g. Hu et al., 2005; Sun, 2005).

The basement lithology of this region is part of the Sino-Korean Achaean shield (Zhang et al., 1998) and is composed primarily of Archean metamorphic rocks including gneiss, phyllite and dolomite, and Lower Paleozoic limestone. South of Wutai Mountain the bedrock comprises Proterozoic metamorphic rocks mainly including biotite-granulite and plagioclase amphibolite. Cenozoic deposits are distributed in the graben and along the valley. Neogene deposits are mainly reddish clays with gravel. Faunas from the reddish clays, such as *Viverra* sp., *Hipparion houfenese*, *Gazella blachi*, *Sinoryx* sp., *Antilospira* and *Palaeotragus* sp., indicate a hot and dry climate (Li et al., 1998). Quaternary deposits are mainly fluviolacustrine deposits in the centers of the basins, whereas alluvial sand and gravel and aeolian loess accumulate at the margins. Pollen and fauna in the Nihewan Formation in the eastern Datong basin indicate that the climate in the Quaternary was cooler than that in the Pliocene (Wang et al., 1996).

3.Methods

Based on satellite image interpretation and field investigation, we mapped and constructed fluvial terrace sequence of the Hutuo River in the basin and gorge segments, combined with sedimentary

characteristics of terrace fill and the identification of the overlying loess-paleosol sequence. Terrace fill and clast lithology are directly observed and logged in the field. The height of terrace above present riverbed was surveyed with a laser rangefinder with a meter accuracy. In addition, we used two handheld GPS units (MobileMapper 6, Magellan Company) to determine the altitude of the top of lacustrine deposits using a differential GPS (DGPS) technique proposed by Stokes et al. (2012). The designed accuracy of the GPS unit is 2.0-3.0 m with a WAAS (wide area augmentation system, a wide area DGPS). In the field, we set one GPS unit as the reference station at a fixed location, and another unit as the mobile station. Both reference and mobile station data are available, and the DGPS results produce a position dilution of precision mean less than 4.5 in altitude. We believe that the accuracy of the altitude for the top of paleolake sediments is less than 5.0 m. Using control points in the 1:50000 topographic maps to calibrate the measurement indicates that the altitude data from this measurement system are reliable. In this paper, fluvial terraces are described from oldest to youngest in relative stratigraphic order.

To determine the age of the terrace sequence, we use numerical dating and the relative age of the overlying loess. It is to note that the age of a fluvial terrace here is the age when the terrace tread was abandoned by the active stream. The overbank sand of the lower terraces (T1-T3) and the overlying loess were dated by TL and OSL. The samples were collected using steel tubes (length ~20 cm, diameter ~5 cm). The tubes were sealed immediately using aluminum foil and tape to retain moisture and avoid daylight exposure. We collected one OSL sample and five TL samples. The OSL sample was assayed by Xulong Wang, State Key Laboratory of Loess and Quaternary Geology, Institute of Earth Environment, Chinese Academy of Sciences. TL samples were tested by Huanzhen Wang, Luminescence Laboratory, Institute of Crustal Dynamics, China Earthquake

Administration. Under weak red light, fine quartz grains(4-11 μm) were separated and the purity was tested by the IRSL scanning until an IRSL/OSL ratio less than 10%. The equivalent dose was determined using fine-grained quartz (4-11 μm) on a Daybreak 2200 automated reader with the single aliquot regenerative-dose prococol initially developed by Zhou and Shackleton (2001). Following the experimental procedures of Lu et al. (2007) and Wang et al. (2010), uranium and thorium contents were determined with Daybreak 583 thick source alpha-counter. The potassium content was measured with flame photometer.

Because the ages of the higher terraces may be beyond the typical range of commonly used luminescence and radiocarbon dating methods (Forman, 1991), the relative age using the loess-paleosol time scale was also adopted. Numerous studies have shown that dustfall has been so persistent since the late Miocene in the Chinese Loess Plateau (e.g. Porter et al., 1992; Qiang et al., 2001) that accumulation of aeolian sediments would have started immediately after the formation of any Pliocene or Pleistocene geomorphic surface. Our field investigations revealed that the sedimentary change from the underlying fluvial deposits to the overlying loess-paleosol section is gradual without an erosion surface between them, indicating that deposition was continuous when the sedimentary environment transformed from subaqueous to subaerial. In this context, the basal ages of aeolian deposits immediately overlying fluvial terraces can be considered as the age of the abandonment of fluvial terraces. This approach has been extensively used in the timing of Quaternary river terraces in the Chinese Loess Plateau (e.g. Sun, 2005; Huang et al., 2011; Pan et al., 2011; Vandenberghe et al., 2011).

The identification of the loess-paleosol units can be based on their distinctive physical

characteristics (e.g. texture, structure, thickness, color and magnetic susceptibility) as well as their stratigraphic position in the regional succession (Sun, 2005; Fang et al., 2007; Zhang et al., 2007). Some prominent paleosol units are widely used as marker lines in the Chinese loess chronology. For example, paleosol S_5 comprises three well-developed soils correlated to MIS 13-15 dated to 580-479 ka, respectively (Fig. 3) (Kukla and An, 1989; Ding et al., 2002), and palaeosol S_1 consists of three distinctive paleosol subunits (S_{1-1}, S_{1-3} and S_{1-5}) alternating with two loess subunits (S_{1-2} and S_{1-4}). It developed during the MIS 5 that was dated to 127-73 ka (Fig. 3), among which paleosol subunits S_{1-5} developed during the MIS 5e that was dated to 127-117 ka (Kukla and An, 1989; Ding et al., 2002). Gray-black palaeosol S_0 formed during MIS 1 and is dated to 11-3.1 ka by radiocarbon and OSL dating (Fig. 3) (Zhang et al., 2007). In this study, we use texture, structure, color and magnetic susceptibility to identify the loess-paleosol units. In addition, some units were dated by TL dating as a supplementary constraint in age. Magnetic susceptibility of loess sequence mantled on river terraces was measured to determine the accurate thickness of each unit using a Bartington MS2 bridge at a 3-5 cm interval in the field after removing the 5-cm-thick surface of natural exposure to avoid the effect of the weathered soil.

4. Terrace sequence in the basin segment of the Hutuo River

Field investigations indicate that the Hutuo River was limited in a ~10-km-wide basin and three terraces are developed in the basin segment (Fig. 2a). T2 is the most widely distributed in the basin, and all the towns are located on it. T1 is distributed adjacent to the present river channel and is the site of farmlands and some villages. T3, the oldest terrace, is sparsely preserved (Fig. 4). We choose two sites where terraces are well preserved to illustrate the characteristics of fluvial

terraces in the basin segment.

4.1. Sulongkou site

West of Sulongkou, large alluvial fans are developed along the normal faulting-controlled mountain frontal areas, and the fluvial sediments show erosional contact with alluvial fan and loess platform (Fig. 5). On the north valley side of the Hutuo River, T3 is characterized by relic of fluvial sand due to human excavation. While on the south valley side, T3 is well preserved and is ~25 m high above riverbed. The terrace fill is composed by channel facies of cross-bedded grayish-black fine gravel in the lower part and overbank facies of laminated gray-yellow sand and silt with horizontal bedding in the upper part. Atop fluvial sediments, there is an overlying layer of reddish paleosol (S_1) covered by yellowish loess (L_1) (Fig. 6). In the lower part of S_1, a thin layer of pedogenic carbonate nodules (Fig. 6b) formed due to leaching during the formation of S_1, suggesting that T3 was abandoned at the formation stage of S_1. No T2 terrace is developed on the river valley near Sulongkou (Fig. 5). T1 is 4 m high above present riverbed, and its terrace fill consists of horizontally bedded fluvial fine sand and silt.

4.2. Jiehepu site

At Jiehepu Village south of Yuanping County (Fig. 2a), where the Hutuo River cuts across the southernmost end of Wutai Mountain and forms a relatively narrow channel. A complete terrace sequence in the basin segment is best preserved at this site.

T3, 26 m high above riverbed, is developed on the west valley side, and is expressed by a fluvial platform with the altitude of ~820 m (Fig. 7a). North of Jiehepu, the overlying loess on T3 is

completely removed due to human modification. The terrace fill includes five sedimentary units from bottom to top (Fig. 7b). Unit 1 is composed by from cross-bedded brownish-yellow coarse sand filled with fine gravel in the lower part, to horizontally bedded brownish-yellow fine sand in the middle part, and to yellowish sandy silt with horizontal bedding in the upper part. Unit 2 consists of coarse to fine sand. Unit 3 includes a bottom brownish-yellow coarse sand with cross-bedding, a middle horizontally-bedded brownish fine sand, and an overlying grayish sandy silt. Unit 4 comprises a bottom consisting of grayish cross-bedded fine gravel filled with coarse sand, a middle fine sand and silt with horizontal bedding, and a top grayish horizontally bedded sandy silt. Unit 5 is composed of brownish-yellow coarse sand and small gravel with cross-bedding overlain by a yellowish fine sand and silt with horizontal bedding.

In a sand excavation west of Jiehepu, terrace fill of T3 is composed of channel facies of grayish-yellow sand and gravel with cross-bedding and horizontal bedding in the lower part and overbank facies of horizontally bedded fine sand and silt in the upper part (Fig. 7d). An overlying loess-paleosol sequence including brownish-red paleosol layers blankets the fluvial deposits. The measurement of magnetic susceptibility of the overlying loess section (Fig. 7e) reveals that three paleosol subunits are separated by two subunits of brownish loess filled with small carbonate nodules. A TL sample collected in the middle of this paleosol unit yielded an age of 103.45±8.79 ka (Fig. 7e). The above evidence demonstrates that the overlying paleosol unit corresponds to S_1, and the lowest paleosol subunit is $S_{1\text{-}5}$ (Fig. 7d).

T2, 9 m high above riverbed, is well preserved on the east valley side of the modern channel (Fig. 7a). The terrace fill is composed of horizontally bedded yellow fine sand. In the overlaying loess,

a grayish-black paleosol can be identified. The magnetic susceptibility curve of the loess section (Fig. 7c) and the comparison with the loess results in the Xin-Ding basin (Zhang et al., 2007) indicate that the paleosol is probably S_0, and the loess above fluvial sand is L_1. An OSL sample taken from the top of fluvial fine sand yielded an age of 21.3±1.1 ka (Fig. 7a). This date provides a maximum age of T2 at ~21 ka, consistent with the age range of the overlying loess (L_2) (Kukla and An, 1989; Ding et al., 2002).

T1, 3-4 m high above riverbed, is widely distributed on both valley sides of the Hutuo River. The terrace fill is composed mainly of grayish-yellow fine sand with horizontal bedding. A TL sample taken from the top sandy silt 50 cm below the surface of T1 was dated at 5.98±0.51 ka (Fig. 7b). This date provides a maximum age of T1 at ~6 ka.

In fact, numerous preliminary studies have been done on the age of this section of T3 in Fig. 7b. Li and Liang (1965) inferred that the deposits accumulated during the Early Pleistocene according to sedimentary characteristics. The Hydrogeological Team of Geological Bureau of Shanxi Province (1977) divided this section into three parts possibly formed in Early, Middle and Late Pleistocene, respectively. Paleomagnetic results by Wang et al. (1996) indicated that the whole section deposited during the Brunhes normal polarity, and they proposed the deposition of this sediments during the Middle-Late Pleistocene. We collected a TL sample from the top of Unit 1 of this section. It was dated at 117.37±9.98 ka (Fig. 7b), consistent with the inference of Wang et al. (1996). From the section west of Jiehepu (Fig. 7d), T3 is overlain by $S_{1\text{-}5}$, ranging in age from 117 to 127 ka (Kukla and An, 1989; Ding et al., 2002). It suggests that T3 was formed in the period of the formation of $S_{1\text{-}5}$, consistent with our TL result. The above evidence reveals that T3 was

abandoned at 120-130 ka given the uncertainty of dating methods.

In summary, only three terraces are developed in the basin segment. T3 is 23-26 m high above riverbed and was formed at 120-130 ka. T2 is 9-10 m high above riverbed and its maximum age is ~21 ka. T1 is ~4 m high above riverbed and was formed at ~6 ka.

5.Terrace sequence in the gorge segment of the Hutuo River

The drainage divide between the basin and gorge segments is ~1100 m above sea level and is characterized by topographic bedrock ridges close to the basin. Our field observations indicate that fluvial terraces are poorly preserved in the Shihouping-Pingshang transverse valley. Below Pingshang, the river is marked by entrenched meanders. At least five terraces are developed generally on the convex side of the meander. We focus on fluvial terraces at the following three sites for detailed studies.

5.1. Rongjiazhuang site

At Rongjiazhuang Village, the Hutuo River flows from south to north and turns south to generate a big bend; the terraces are exposured on the eastern valley side of the modern channel (Fig. 8a). T5 is 205 m high above present riverbed. Sparse fluvial gravels can be found on the T5 tread (Fig. 8c). Above T5, there is a bedrock platform where no fluvial gravel was preserved (Fig. 8c), suggesting that the platform might be an older erosional terrace. T4 is ~121 m high above riverbed. The terrace fill is characterized by horizontally bedded gray calcite-cemented gravel up to 15 m thick and has an Archean gneiss basement bedrock. Clast lithology of the gravels is mainly limestone and gneiss. The fluvial sediments are mantled by a loess section up to 21 m thick.

Paleosol S_5 can be identified directly on the top of fluvial sediments according to the characteristics of the overlying loess-paleosol sequence (Fig. 8c).

T3 is 46 m high above riverbed and the terrace fill consist primarily of fluvial gravel with a thickness of ~10 m. At the back margin of the terrace, fluvial gravel shows an erosional contact with loess L_2 (Fig. 8b). Atop L_2, there is a brownish-red paleosol unit embracing three reddish subunits and two yellowish subunits, similar to paleosol S_1 at Jiehepu Village (Fig. 7d) and the published loess section in the east part of the Xin-Ding basin (Zhang et al., 2007). We, therefore, infer that T3 was formed in the period of the lowest paleosol subunit ($S_{1\text{-}5}$).

T2 and T1 are 20 m and 5 m high above riverbed, respectively (Fig. 8c). Their fills are fluvial sand and gravel. Rongjiazhuang Village is located on terrace T2 and the loess above the terrace may have been removed due to human excavation.

5.2. Zhaojiazhuang site

At Zhaojiazhuang Village, five terraces are well preserved on the eastern valley side of the Hutuo River (Fig. 9a). T5, 158 m high above riverbed, is an erosional terrace (Fig. 9b). T4 is 104 m high above riverbed and has a basement of Cambrian limestone. Its sediments are composed of ~10-m-thick calcite-cemented gravel with a general clast size from 5 to 15 cm. A loess-paleosol section up to 30 m thick caps the fluvial sediments, and the lowest unit is identified to be paleosol S_5 (Fig. 9b).

T3 is 51 m high above riverbed. The terrace fill consists mainly of imbricate gray semi-cemented gravels up to 7 m thick with clast size ranging from 2 to 10 cm (Fig. 9c). Clast lithology is mainly

limestone and gneiss. The magnetic susceptibility curve of the overlying loess indicates that the three reddish paleosol subunits represent S_{1-1}, S_{1-3} and S_{1-5}, respectively (Fig. 9c).

T2 and T1 are 29 m and 7 m high above riverbed, respectively. Their terrace fill is composed of fluvial gravel (Fig. 9b). Zhangjiazhuang Village is located on T2. Due to human activity, most of the loess on the T2 surface has been removed.

5.3. Lingzidi site

At Lingzidi Village, five terraces forms on the eastern valley side of the modern Hutuo River (Fig. 10a). The terraces above T3 have a basement of Archean schist and gneiss bedrock (Fig. 10e). T5 is 103 m high above riverbed. Its terrace fill is composed of fluvial gravel up to 10 m thick, but is not overlain by loess (Fig. 10e), implying that it has probably undergone erosion after the formation of T5. T4 is 82 m high above riverbed and its terrace fill consists primarily of a unit of ~18-m-thick gray fluvial gravel. Only a 2-m-thick paleosol relic with interlayers of carbonate nodules covers the fluvial sediments of T4 (Fig. 10e).

T3 is 49 m high above riverbed and the terrace fill comprises gray fluvial sand and gravel up to 7 m thick. Clast lithology is mainly limestone and gneiss. The loess mantled on T3 is about 8 m thick with a basal paleosol S_1 (Fig. 10e). One TL sample collected from fine sand in the top of fluvial sediments yielded an age of 130.43±11.09 ka (Fig. 10e). T2 and T1 are 22 and 5 m high above riverbed, respectively. Their fills are composed of fluvial gravels filled with sand. Additionally, T2 gravels are overlain by a ~1.5-m-thick loess L_1 and the lowest part of the overlying loess L_1 was dated by TL at 20.51 ± 1.74 ka (Fig. 10e), suggesting that the abandonment

of T2 occurred prior to this date.

Also, T3 and T2 are developed north of Lingzidi Village (Fig. 10a). Fluvial deposits of T3 have a base of loess L_2 and are mantled by paleosol S_1 including three distinct reddish paleosol subunits (Fig. 10b), showing that deposition of fluvial sediments of T3 began during the accumulation of loess L_2 and ended in the beginning of the formation of paleosol S_1. T2 has a similar height to terrace T2 at Lingzidi Village. The erosion surface at the back margin of T2 indicates that Hutuo River incised fluvial gravels of terrace T3, and subsequently deposited the fluvial sediments of terrace T2 (Fig. 10c). Terrace T2 is capped by the loess including a grayish-black paleosol (Fig. 10c). The magnetic susceptibility curve of the overlying loess (Fig. 10d) and the comparison with the loess-paleosol section in the Xin-Ding basin (Zhang et al., 2007) demonstrate that the paleosol is S_0. A TL sample taken from fine sand atop fluvial sediments of T2 yielded an age of 26.88 ± 2.28 ka (Fig. 10c).

In summary, five terraces are widely developed in the gorge segment. T5 is an erosional terrace and is ~150-200 m high above riverbed. Only sparse fluvial gravels are preserved on it, that makes it hard to collect the material for the dating of this terrace. T4 is 100-121 m high above riverbed, and its fluvial sediments consist mainly of calcite-cemented clasts capped by paleosol S_5, with the age range of 580-479 ka (Kukla and An, 1989; Ding et al., 2002), suggesting that the maximum age of T4 is ~600 ka. T3 is 49-54 m high above riverbed and is composed primarily of poorly cemented cross-bedded gravel. The overlying $S_{1\text{-}5}$, with the age range of 127-117 ka (Kukla and An, 1989; Ding et al., 2002), and TL dating of the top fluvial deposits indicate that T3 was formed at 120-130 ka. T2 is 20-29 m high above riverbed and is mantled by L_1. TL dating of its top fluvial

sand provides a maximum age of T2 at ~26 ka. T1 is 5-7 m high above riverbed. Radiocarbon dating of a peat layer embedded in the middle of the T1 fluvial sediments north of Pingshang yielded the age of 7.640 ± 0.115 ka (Cheng and Ran, 1981). This date may be somewhat older than the T1 age, but we can infer that the maximum age of T1 is ~7 ka according to the results of the T1 age in this region (Ren and Zhang, 2006; Zhang et al., 2007).

6.Fluvial geomorphology along the Qingshui River

Satellite imagery shows that a tributary of the Hutuo River (named Qingshui River) joins the Hutuo River at Pingshang Village (Figs. 2a and 11). Field investigations show that at least fluvial four terraces are well preserved along the Qingshui River.

At Hujiazhuang Village, four terraces are developed on the northern valley side of the modern channel (Fig. 12). T4 is 73 m above present riverbed and its terrace fill comprises the calcite-cemented gravel. The fluvial sediments of T4 are mantled by a remnant of Middle-Pleistocene loess. T3 is 42 m above present riverbed. Terrace fill of T3 consists of horizontally bedded fluvial gravels up to 6 m thick and is capped by a loess section with the basal paleosol S_1 (Fig. 12). T4 and T3 have a limestone basement bedrock. T2 and T1 are 15 m and 4 m above riverbed, respectively. Their terrace fill consists mainly of fluvial gravels filled with fine sand. These terraces have flat and wide treads, and are currently occupied by farmland and road (Fig. 12).

7.Paleolake deposits in the Xin-Ding basin

In the Xin-Ding basin, the deposits related to the paleolake is mostly buried by loess and fluvial

sediments. Drilling data in the Dingxiang and Dongye subbasins shows that the lacustrine sediments unconformably overlay the Neogene red clay (Fig. 13), showing that the Xin-Ding basin was occupied by a paleolake since the Early Pleistocene. This accords with the major period of paleolake expansion in the Shanxi rift system (Xu et al., 1993; Li et al., 1998).

In addition, two exposures of paleolake deposits were found in our field investigation. One site is located at Tanglingang Village, south of Yuanping (Fig. 2a). The lacustrine sediments consist of compacted yellowish-green clay and silt with fine sand interlayers (Fig. 14a). Above the lacustrine sediment is horizontally bedded ~1-m-thick brown fluvial sand overlain by a 1.5-m-thick late Quaternary yellowish loess. The overlying loess section is not complete probably due to human activity that we can determine the age of the loess based on the time scale of the loess-paleosol sequence. The top of fluvial sand is ~28 m high above the present riverbed south of Tanglingang (Fig. 14b), suggesting that this fluvial sand likely corresponds to T3 at Jiehepu (Fig. 7). The transition from paleolake to fluvial facies represents that fluvial deposition by the Hutuo River was dominant at this site after the paleolake, implying that the shrinkage of the paleolake occurred somewhat earlier than the fluvial sand of T3. Another site lies south of Dongye. The lacustrine sediments are capped by secondary loess and late Quaternary loess (Fig. 15a). We measured the altitude of the top of paleolake deposits at two sites and obtained a similar altitude of ~800 m.

Generally, the border of a lake is generally the site where the altitude of the sediments is close to the highest level of the lake and the sediments are the thinnest. From the border to the lake center, the lake sediments get thicker. At the second exposure, the paleolake sediments become thicker from south to north. At the southernmost side, the sediments are very thin and may be close to the

margin of the paleolake sediments. In addition, the paleolake sediments underlie the loess, suggesting that the high level of the paleolake took place in the period of the loess accumulation. The secondary loess (Fig. 15a) is the reworked loess probably by the lake water, possibly combined with tributaries draining the paleolake. The ~2-3 m thick secondary loess may represent the highest site of the disturbance by the paleolake water. So we infer that the site may be very close to the border of the paleolake and the top of lacustrine sediments at this site likely represents the highest level of the Xin-Ding paleolake before the breach. The extent of the Xin-Ding paleolake before the breach is outlined in Fig. 16b, indicating that the Dingxiang, Dongye subbasins and a part of the Yuangping subbasins were in the lake environment. This result is consistent with the inference of Chen (1983) determined from drilling data in the Xin-Ding basin.

8.Paleogeographic reconstructions

Terrace sequence of the Hutuo River indicates that terraces T1-T3 are widely distributed in the basin and gorge segments and their ages are roughly concurrent, implying that the Shihouping-Pingshang transverse drainage was created prior to the formation of terrace T3. However, T4 and older terraces can be found in the gorge segment, but not in the basin segment (Fig. 4), indicating that the creation of this transverse drainage occurred after the formation of terrace T4. The reconstruction of terrace sequence indicates that terraces T3 and T4 were abandoned at 120-130 ka and ~600 ka, respectively. Thus, the formation of the Shihouping-Pingshang transverse drainage happened between ~600 ka and ~130 ka. In other words, the breach of the Xin-Ding paleolake took place during the Middle Pleistocene.

Terraces older than T3 are also developed along the Qingshui River (Fig. 12). Based on the

distribution of the Tangxian surface and river morphology, the ancestral Qingshui River might pass from the present-day Hutuo channel below Pingshang prior to the creation of the Shihouping-Pingshang transverse drainage. In addition, field observations show a unit of calcite-cemented gravels similar to the T4 gravels is sparsely preserved in the transverse valley, suggesting that there are small paleoflows before the Hutuo River incised into the Xin-Ding basin (Figs. 11a and 15b).

Combined with previous studies (Willis and Blackwelder, 1907; Li and Liang, 1965; Wang et al., 1996; Li et al., 1998), three stages of paleogeographic reconstructions are made for river evolution in the upper reach of the Hutuo drainage system Since the Pliocene (Fig. 16).

During the Pliocene, the ancestral Hutuo River flowed southwards into the Taiyuan Basin and finally joined the Fenhe River, and the ancestral Qingshui River flowed along the present Hutuo channel (Fig. 16a).

During the Early Pleistocene, due to the uplift near the Shilingguan Col shown in numerous studies (Xu et al., 1993; Li et al., 1998; Zhang et al., 1998; Zhang et al., 2007), the ancestral Hutuo River had to abandon its former course and turned eastward to generate the paleolake in the south part of the Xin-Ding basin. The tributaries of the ancestral Hutuo River drained the paleolake (Fig. 16b). In this stage, the ancestral Qingshui River remained to keep its previous channel and produced T4 and older terraces. This drainage pattern might be kept untill the Middle Pleistocene.

Since the Late Pleistocene, the Shihouping-Pingshang transverse drainage has been established, and the Xin-Ding paleolake has been breached. The catchment of the paleolake merged into the

ancestral Qingshui River. The catchment of the paleolake is evidently larger than that of the ancestral Qingshui River above Pingshang, that resulted in the formation of the present drainage framework of the Hutuo River. The basin drainage segment became the stem of the upper reach of the Hutuo drainage, and the Qingshui River was as one of its tributaries (Fig. 16c). After that, the Hutuo River entered the Xin-Ding basin and generated terraces T3-T1.

9.Mechanisms for the creation of transverse drainage

After the reconstruction of the long-term drainage evolution of the upper reach of the Hutuo River, the factors attributed to the formation of the Shihouping-Pingshang transverse drainage need to be considered. Generally, transverse drainage is related to the following mechanisms: antecedence, superimposition, overflow, and capture (Stokes and Mather, 2003; Douglass and Schmeeckle, 2007; Douglass et al., 2009).

(1) *Antecedence*

For antecedence to develop, a stream has the capacity to erode into a uplifting bedrock structure and continue to transport deposit downstream without periods of prolonged aggradation (e.g. Stokes and Mather, 2003; Douglass et al., 2009). Namely, it requires fluvial incision to keep up with uplift. Tectonic uplift in the study area has taken place along the boundary faults since the Pliocene (Xu et al., 1993). But for antecedence to work a fluvial link between the Xin-Ding basin and ancestral Qingshui River would need to have been there from the Pliocene onwards. There is no geomorphic evidence for antecedence along the reach of the transverse drainage (Fig. 11b). This is not also in agreement with the inference based on fluvial terrace sequence. Thus,

antecedence is not applicable to the creation of transverse drainage at this site.

(2) *Superimposition*

Superimposition requires that a stream flow over a covermass that buries a relatively resistant bedrock structure (Douglass and Schmeeckle, 2007). The covermass can comprise alluvium, erodible bedrock, or lacustrine deposits. For superimposition to take place, the stream needs to transport both the bedrock eroded from the transverse gorge and the alluvial, lacustrine, or uncomformable bedrock material that once buried the bedrock structure. In other word, this mechanism would require the limestone basement of the Xizhou Mountain to be overlain by a thin covermass of Pliocene-Pleistocene age. A southeastward-flowing stream would then need to remove this covermass and to superpose itself atop and across the basement of the Xizhou Mountain. Superimposition is an unlikely mechanism for the creation of this transverse gorge for the following reasons. First, there is no evidence for any remnants of Pliocene-Pleistocene deposits on the Xinzhou basement in the area of the transverse reach or across the Xinzhou Mountain (Fig. 11a). It is therefore impossible that the Xinzhou basement was buried by Pliocene-Pleistocene deposits. Second, if the transverse drainage was dissected in the Early Pleistocene or even earlier, terraces older than T4 or even the Tangxian surface would have been developed along the transverse reach.

(3) *Overflow*

A stream becomes ponded in an interior-drained basin and eventually overspill at the lowest point of the basin rim. A river must have been ponded in a lake prior to the formation of an overflow

transverse drainage. Blackwelder (1934) proposed that the overflow of a paleolake is mainly associated with climate-related lake-level rise. But the study on the Linfen paleolake south of the Xin-Ding basin (Fig. 1) indicated that no prominent expansion of the lake level due to climate change occurred during the Middle Pleistocene in the study area and even the palaeolake expassion due to tectonic uplift caused only 40-60 m of the lake level rise (Hu et al., 2005). It is hard to lead to the overflow of the divide over 200 m high above paleolake level. The drilling data in the Dongye subbasin (Fig. 13) indicate that a paleoflow draining the Dongye subbasin related to the cemented gravels at the southern margin always coexisted with the paleolake and height of cemented gravels is higher than the paleolake level, implying that no paleolake overflow occurred at the transverse gorge. In addition, in extensional tectonic settings, several transverse gorges can generally develop along the same river via overflow (Meek and Douglass, 2001; Douglass et al., 2009). In the field investigation there is no evidence of another transverse drainage between the ancestral Qingshui River and Xin-Ding basin (Fig. 11b). Overflow is therefore an unlikely driving mechanism for the creation of the transverse gorge in this case.

(4) *Piracy*

The piracy or capture of a stream occurs when part of a channel's previous course changes to that of another stream. The point of capture can occur across a topographic high dividing two drainage systems, therefore, leading to a pirated transverse drainage (Douglass et al., 2009). Stream piracy happens when the soon-to-be captured stream erodes and flows across an intervening interfluve into a drainage system.

In this case, the Shihouping-Pingshang transverse gorge connects the Xin-Ding and ancestral

Qingshui drainage systems. As mentioned above, the cemented gravels similar to terrace T4 are distributed along the transverse gorge. According to the study of Cheng (1983), the roundness of clasts of the cemented gravels between Shihouping and Pingshang is distinctly lower than that along the Qingshui and Hutuo valleys. Moreover, clast lithology of the cemented gravels in the transverse valley is dominantly limestone, whereas that along the Qingshui River comprises limestone and metamorphic rocks. From the geological map (Fig. 11a), the transverse drainage flows mainly in the area of limestone, whereas the Qingshui River and the upper reach of Hutuo River cut across the region of limestone and metamorphic rocks. The above evidence indicates that the gravel in the Shihouping-Pingshang transverse valley is evidently localized deposition.

Interestingly, between the divide and Shihouping Village, clast imbrication of this cemented gravels consistently dip southeast, implying a northwestward-flowing paleostream, opposite to the flow direction of the current Hutuo River (Figs. 11a and 15b), whereas clasts of the gravels between the divide and Pingshang dip generally northwest, suggesting a southeastward-flowing paleostream (Fig. 11a). The opposite paleoflow directions on both sides of the divide suggest that prior to the creation of the transverse gorge, the ancestral Qingshui and Xin-Ding drainage systems were not connected. Under the joint ongoing headwater erosion of the southeastward- and northwestward-flowing paleostreams decreased the divide and finally resulted in the capture of the northwestward-flowing paleostream by the southeastward-flowing paleostream and the breach of the Xin-Ding paleolake.

In this sense, drainage piracy is the driving mechanism for the creation of the Shihouping-Pingshang transverse drainage. Certainly, we cannot completely rule out the

possibility that when the divide decreases to be lower than the paleolake level, the overflow would promote the incision of the divide and accelerate the formation of the transverse drainage. Douglass and Schmeeckle (2007)'s physical model on the piracy mechanism indicated four subtypes: aggradation, lateral erosion, sapping, and headward erosion. The case of the upper reach of the Hutuo drainage supports the type of headward erosion that depends on the lowering of base level.

10. Controls of base level lowering

Generally, the change of base level can be attributed to intrinsic and extrinsic factors (Mather, 2000). The intrinsic controls are primarily associated with bedrock lithology and geologic structure (Bull, 1991). River patterns generally have a close relationship to structure of the underlying bedrock. Drainages will adjust to the underlying bedrock structure during fluvial incision as shown in the studies by Harvey and Wells (1987) and Stokes et al. (2008). In the area of the Shihouping-Pingshang transverse drainage, bedrock lithology is approximately uniform. All the structures are dominantly northeast-trending, and no northwest-trending structure exists (Fig. 2a). Thus, we exclude the intrinsic factors.

Extrinsic factors includes eustatic sea-level variation, tectonism, and climate change (e.g. Harvey and Wells, 1987; Bull, 1991; Stokes and Mather, 2003; Maher et al., 2007; Ghoneim et al., 2012). Because the study area is over 400 km far from the sea, the impact of eustatic sea-level drop on the lowering of base level of the upper Hutuo drainage system can be negligible. The discussion below will consider the effects of climate change versus tectonic activity for the base level lowering in the formation of the Shihouping-Pingshang transverse drainage.

(1) *Climate change*

Climate fluctuation exerts effects on Quaternary fluvial evolution through its influence on the sediment/discharge ratio (Bull, 1991). During the Quaternary, fluvial aggradation is generally considered to have occurred during glacial periods (Starkel, 2003), while the lowering of base level occurs and results in incision during interglacials (e.g. Vandenberghe, 2003) or during glacial–interglacial transition periods (e.g. Bridgland and Westaway, 2008). Here, climate change is an unlikey controlling factor for the base level lowering in this case.

First, the impact of climate change is generally regional, but not localized. If the lowering of base level was driven by climate change, consequent incision and terraces would have been observed along the drainages of this region. However, incision only occurs in the Shihouping-Pingshang transverse drainage, but not along the adjacent Qingshui and Hutuo valleys.

Second, based on changes in the facies of the lacustrine sediments in the Linfen paleolake south of Xin-Ding basin (Fig. 1), Hu et al. (2005) proposed that climate changes in the Pleistocene could result in only 2-3 meters of the lake level fluctuation when tectonic uplift was relatively quiescent. It is hard to imagine that the incision due to this small lowering of base level can cut across the divide over 200 m high between the Xin-Ding paleolake and ancestral Qingshui drainage (Fig. 4). In addition, the climate change will not provide a sustained base level lowering mechanism to allow headward erosion and the creation of the Shihouping-Pingshang transverse drainage as illustrated by Stokes et al. (2012).

(2) *Tectonic activity*

Active tectonics in form of differential uplift and subsidence can lead to fluvial incision by steepening geomorphic gradients and increasing the stream power of the fluvial system (Holbrook and Schumm, 1999; Burbank and Anderson, 2011). In this study area, active activity by differential uplift has been a primary factor in the generation of topography (Xu et al., 1993; Li et al., 1998; Zhang et al., 2007). Since the Pliocene, the Shanxi rift system underwent extension (Xu and Ma, 1992; Zhang et al., 1998). The boundary faults of the Xin-Ding graben is dominated by normal faulting that accompanied episodic uplift of the mountains (Zhang et al., 2007). Along the Xizhou fault, distinctive alluvial fans and displaced geomorphic features in the frontal area suggested a strong tectonic uplift and tilting of the Xinzhou Mountain block (Xu et al., 1993; Li et al., 1998).

On the both sides of the drainage divide at the Shihouping-Pingshang transverse stream, there is a distinctive difference in topographic gradient. To the north of the divide, the height increases ~300 m in the distance of ~4 km, whereas to the north, the increase of height is up to ~400 m in the distance of ~8 km. The steeper gradient on the northern slope is due to tectonic tilting of the Xizhou fault (Fig. 4).

The tilting of the Xizhou Mountain block would have enhanced stream power and changed local base level of the two drainage systems prior to the breach of the transverse gorge. As illustrated above, on the northern slope, the cemented gravels show evidence of a northwestward-flowing localized paleostream draining the paleolake with the base level of the paleolake, whereas on the southern slope, the southeastward-flowing paleotributary of the ancestral Qingshui River (Fig. 11a) took the riverbed of the ancestral Qingshui River as its base level. Fluvial terrace data indicates

that the T4 terrace was probably its riverbed prior to the capture. The level of the Xin-Ding paleolake prior to the breach is ~800 m in altitude. The base level on the southern slope is ~50 m lower than that on the northern slope (Fig. 4), suggesting a bigger capacity of incision on the south slope. In addition, the catchment area of the southeastward-flowing paleostream is apparently larger than that of the northwestward-flowing one (Fig. 11a). Under the same climate condition, the southeastward-flowing paleotributary would have more discharge. Therefore, the southeastward-flowing paleostreams would have more stream power for headward erosion.

Based on the above illustration, differential uplift and associated tilting of the Xizhou Mountain block during the Middle Pleistocene have resulting in the lowering of the local basel level. The southeastward-flowing paleotributary with a lower base level had a stronger headward incision to capture the northwestward-flowing paleostream at the expense of the Qingshui River and finally result in the creation of the transverse drainage and breach of the Xin-Ding paleolake.

In fact, localized tectonism can be an important mechanism for localized incision and drainage reorganization. The type of drainage evolution mainly driven by differential uplift by localized tectonic activity have been found in other areas of the world, for example, the Aguas and Feos river systems, southeast Spain (Harvey and Wells, 1987), the Mississippi River (Schumm et al., 1994), the River Dades, south-central Morocco (Stokes et al., 2008), and the Zagros fold-and-thrust belt of Fars province, Iran (Walker et al., 2011).

11. Conclusions

1) Based on field investigations, numerical dating and the relative age of the overlying loess,

five fluvial terraces (T5-T1) are developed along the upper reach of the Hutuo River, amongst which terraces T4-T1 were formed concurrently at ~600 ka, ~120-130 ka, ~21-26 ka and ~6-7 ka, respectively. Only three younger terraces (T3-T1) are developed in the basin segment, and older terraces are distributed in the gorge segment.

2) The creation of the Shihouping-Pingshang transverse drainage and breach of the Xin-Ding paleolake occurred between ~600 ka and ~130 ka.

3) Three stages of paleogeographic reconstructions are established for river evolution in the upper reach of the Hutuo drainage system Since the Pliocene.

4) The mechanism for the creation of the Shihouping-Pingshang transverse drainage is via river capture of paleostreams on both sides of the drainage divide.

5) Localized differential uplift and associated tilting of the Xizhou Mountain block during the Middle Pleistocene have caused the lowering of the local base level finally resulting in the creation of the transverse drainage and breach of the Xin-Ding paleolake.

Acknowledgments

This work was supported by the National Science Foundation of China (grant No. 40972143) and Institute of Crustal Dynamics, China Earthquake Administration Research Fund (grant No. ZDJ2013-23). We thank Zhongxian Huang, Martin Stokes and another anonymous reviewer for thoroughly reviewing the manuscript.

References

Bishop, P., 1995. Drainage rearrangement by river capture, beheading and diversion. *Progress in Physical Geography*, 19(4): 449-473.

Blackwelder, E., 1934. Origin of the Colorado River. *Geological Society of America Bulletin*, 45(3): 551-566.

Bridgland, D. and Westaway, R., 2008. Climatically controlled river terrace staircases: A worldwide Quaternary phenomenon. *Geomorphology*, 98(3-4): 285-315.

Bridgland, D.R. et al., 2012. The River Orontes in Syria and Turkey: Downstream variation of fluvial archives in different crustal blocks. *Geomorphology*, 165–166(0): 25-49.

Bull, W.B., 1991. Geomorphic responses to climatic change. Oxford University Press, New York, 326 pp.

Burbank, D.W. and Anderson, R.S., 2011. Tectonic geomorphology (Second edtion). Wiley-Blackwell, 246-251 pp.

Cheng, S., 1983. Discussion on river capture of Qingshui River and Hutuo River. *Journal of Heibei College of Geology*, 22(2): 41-53 (in Chinese).

Cheng, S. and Ran, Y., 1981. Hutuo river terraces in Taihang canyon section and Quaternary tectonic movement. *Seismology and Geology*, 3(1): 29-39 (in Chinese with English abstract).

Clark, M.K. et al., 2004. Surface uplift, tectonics, and erosion of eastern Tibet from large-scale drainage patterns. *Tectonics*, 23(1): TC1006.

Cordier, S., Harmand, D., Frechen, M. and Beiner, M., 2006. Fluvial system response to Middle and Upper Pleistocene climate change in the Meurthe and Moselle valleys (Eastern Paris Basin and Rhenish Massif). *Quaternary Science Reviews*, 25(13–14): 1460-1474.

Ding, Z. et al., 2002. Stacked 2.6-Ma grain size record from the Chinese loess based on five sections and correlation with the deep-sea $\delta^{18}O$ record. *Paleoceanography*, 17(3-5): 1-20.

Ding, Z.L., Derbyshire, E., Yang, S.L., Sun, J.M. and Liu, T.S., 2005. Stepwise expansion of desert environment across northern China in the past 3.5 Ma and implications for monsoon evolution. *Earth and Planetary Science Letters*, 237(1–2): 45-55.

Douglass, J., Meek, N., Dorn, R.I. and Schmeeckle, M.W., 2009. A criteria-based methodology for determining the mechanism of transverse drainage development, with application to the southwestern United States. *Geological Society of America Bulletin*, 121(3-4): 586-598.

Douglass, J. and Schmeeckle, M., 2007. Analogue modeling of transverse drainage mechanisms. *Geomorphology*, 84(1–2): 22-43.

Fang, X. et al., 2007. High-resolution magnetostratigraphy of the Neogene Huaitoutala section in the eastern Qaidam Basin on the NE Tibetan Plateau, Qinghai Province, China and its implication on tectonic uplift of the NE Tibetan Plateau. *Earth and Planetary Science Letters*, 258(1-2): 293-306.

Forman, S.L., 1991. Late Pleistocene chronology of loess deposition near Luochuan, China. *Quaternary Research*, 36(1): 19-28.

Ghoneim, E., Benedetti, M. and El-Baz, F., 2012. An integrated remote sensing and GIS analysis of the Kufrah Paleoriver, Eastern Sahara. *Geomorphology*, 139-140: 242-257.

Harvey, A.M. and Wells, S.G., 1987. Response of Quaternary fluvial systems to differential epeirogenic uplift: Aguas and Feos river systems, southeast Spain. *Geology*, 15(8): 689-693.

Hasbargen, L.E. and Paola, C., 2000. Landscape instability in an experimental drainage basin. *Geology*, 28(12): 1067-1070.

Holbrook, J. and Schumm, S.A., 1999. Geomorphic and sedimentary response of rivers to tectonic deformation: a brief review and critique of a tool for recognizing subtle epeirogenic deformation in modern and ancient settings. *Tectonophysics*, 305(1–3): 287-306.

Hu, X., Li, Y. and Yang, J., 2005. Quaternary paleolake development in the Fen River basin, North China. *Geomorphology*, 65(1-2): 1-13.

Huang, C.C., Pang, J., Zha, X., Su, H. and Zhou, Y., 2011. Development of gully systems under the combined impact of monsoonal climatic shift and neo-tectonic uplift over the Chinese Loess Plateau. *Quaternary International*, 263: 46-54.

Hunt, C.B., 1971. Geologic history of the Colorado River: The Colorado River Region and John Wesley Powell. U.S. Geological Survey Professional Paper 669-C, pp. C59–C130.

Hydrogeological Team of Geological Bureau of Shanxi Province, 1977. Manual of hydrogeology in Xinding Basin, Shanxi Province (1: 200,000) (In Chinese).

Kukla, G. and An, Z., 1989. Loess stratigraphy in central China. *Palaeogeography, Palaeoclimatology, Palaeoecology*, 72: 203-225.

Lane, A., 1899. A note on a method of stream capture. *Geological Society of America Bulletin*, 10: 12-14.

Li, J. and Fang, X., 1999. Uplift of the Tibetan Plateau and environmental changes. *Chinese Science Bulletin*, 44(23): 2117-2124.

Li, P. and Liang, Q., 1965. Some new data of river channel change at the upper reach of Hutuo river and Muma river. *Geological Review*, 23(3): 240-241(in Chinese with English abstract).

Li, Y., Yang, J., Xia, Z. and Mo, D., 1998. Tectonic geomorphology in the Shanxi Graben System, northern China. *Geomorphology*, 23(1): 77-89.

Lisiecki, L.E. and Raymo, M.E., 2005. A Pliocene-Pleistocene stack of 57 globally distributed benthic $\delta^{18}O$ records. *Paleoceanography*, 20: doi:10.1029/2004PA001071

Liu, D., 1985. Loess and the Environment (in Chinese). China Ocean Press, Beijing, 481 pp.

Lou, T. and Du, R., 1960. Prelimnary investiagation on drainage evolution in Fenhe Graben, Shanxi (in Chinese). *Acta Geographica Sinica*, 26(3): 155-164.

Lu, Y., Wang, X. and Wintle, A.G., 2007. A new OSL chronology for dust accumulation in the last 130,000 yr for the Chinese Loess Plateau. *Quaternary Research*, 67(1): 152-160.

Lucchitta, I., 1972. Early history of the Colorado River in the Basin and Range Province. *Geological Society of America Bulletin*, 83(7): 1933-1948.

Maher, E., Harvey, A.M. and France, D., 2007. The impact of a major Quaternary river capture on the alluvial sediments of a beheaded river system, the Rio Alias SE Spain. *Geomorphology*, 84(3): 344-356.

Mather, A.E., 2000. Adjustment of a drainage network to capture induced base-level change: an example from the Sorbas Basin, SE Spain. *Geomorphology*, 34(3–4): 271-289.

Mayer, L., Menichetti, M., Nesci, O. and Savelli, D., 2003. Morphotectonic approach to the drainage analysis in the north Marche region, central Italy. *Quaternary International*, 101: 157-167.

Meek, N. and Douglass, J., 2001. Lake overflow: An alternative hypothesis for Grand Canyon incision and development of the Colorado River. In: R.A. Young and E.E. Spamer (Editors), Colorado River Origin and Evolution. Grand Canyon Association, Grand Canyon, AZ, pp. 199-204.

No. 601 Geological Team of Geological Bureau of Shanxi Province, 1960. Borehole data for

Hydrogeology in Dongye subbasin (In Chinese).

Oberlander, T., 1985. Origin of drainage transverse to structures in orogens. In: J.T. Hack (Editor), Tectonic Geomorphology, pp. 155-182.

Pan, B., Hu, Z., Wang, J., Vandenberghe, J. and Hu, X., 2011. A magnetostratigraphic record of landscape development in the eastern Ordos Plateau, China: Transition from Late Miocene and Early Pliocene stacked sedimentation to Late Pliocene and Quaternary uplift and incision by the Yellow River. *Geomorphology*, 125(1): 225-238.

Peltzer, G., Tapponnier, P., Zhitao, Z. and Qin, X.Z., 1985. Neogene and Quaternary faulting in and along the Qinling Shan. *Nature*, 317(6037): 500-505.

Porter, S.C., An, Z. and Zheng, H., 1992. Cyclic Quaternary alluviation and terracing in a nonglaciated drainage basin on the north flank of the Qinling Shan, central China. *Quaternary Research*, 38(2): 157-169.

Qiang, X.K., Li, Z.X., Powell, C.M. and Zheng, H.B., 2001. Magnetostratigraphic record of the Late Miocene onset of the East Asian monsoon, and Pliocene uplift of northern Tibet. *Earth and Planetary Science Letters*, 187(1–2): 83-93.

Ren, J. and Zhang, S., 2006. A tectonic movement during the later stage of late Pleistocene epoch in the Xinding basin. *Seismology and Geology*, 28(3): 487-496 (in Chinese with English abstract).

Schumm, S., Rutherfurd, I. and Brooks, J., 1994. Pre-cutoff morphology of the Lower Mississippi River. In: S.A. Schumm and B.R. Winkley (Editors), The variability of large alluvial rivers American Society of Civil Engineers, New York, pp. 13-44.

Simpson, G., 2004. Role of river incision in enhancing deformation. *Geology*, 32(4): 341-344.

Starkel, L., 2003. Climatically controlled terraces in uplifting mountain areas. *Quaternary Science Reviews*, 22(20): 2189-2198.

Stokes, M., 2008. Plio-Pleistocene drainage development in an inverted sedimentary basin: Vera basin, Betic Cordillera, SE Spain. *Geomorphology*, 100(1–2): 193-211.

Stokes, M., Cunha, P.P. and Martins, A.A., 2012. Techniques for analysing Late Cenozoic river terrace sequences. *Geomorphology*, 165–166: 1-6.

Stokes, M. and Mather, A.E., 2003.

Almanzora, Betic Cordillera, Southeast Spain. *Geomorphology*, 50(1–3): 59-81.

Stokes, M., Mather, A.E., Belfoul, A. and Farik, F., 2008. Active and passive tectonic controls for transverse drainage and river gorge development in a collisional mountain belt (Dades Gorges, High Atlas Mountains, Morocco). *Geomorphology*, 102(1): 2-20.

Sun, J., 2005. Long-term fluvial archives in the Fen Wei Graben, central China, and their bearing on the tectonic history of the India-Asia collision system during the Quaternary. *Quaternary Science Reviews*, 24(10-11): 1279-1286.

Twidale, C., 1966. Chronology of denudation in the southern Flinders Ranges, South Australia. *Transactions of the Royal Society of South Australia*, 90(1): 3-28.

Twidale, C.R., 2004. River patterns and their meaning. *Earth-Science Reviews*, 67(3): 159-218.

Vandenberghe, J., 2003. Climate forcing of fluvial system development: an evolution of ideas. *Quaternary Science Reviews*, 22(20): 2053-2060.

Vandenberghe, J., Wang, X. and Lu, H., 2011. Differential impact of small-scaled tectonic movements on fluvial morphology and sedimentology (the Huang Shui catchment, NE Tibet Plateau). *Geomorphology*, 134(3–4): 171-185.

Walker, R.T., Ramsey, L.A. and Jackson, J., 2011. Geomorphic evidence for ancestral drainage patterns in the Zagros Simple Folded Zone and growth of the Iranian plateau. *Geological Magazine*, 148(5-6): 901-910.

Wang, N. et al., 1996. The sediment and structual landform of Shanxi rift system in the Cenozoic (in Chinese). Science Press, Beijing, 400 pp.

Wang, P., Jiang, H., Yuan, D., Liu, X. and Zhang, B., 2010. Optically stimulated luminescence dating of sediments from the Yellow River terraces in Lanzhou: tectonic and climatic implications. *Quaternary Geochronology*, 5(2): 181-186.

Wang, Z., 1926. The instruction of the 1: 1000,000 Chinese geological map (Taiyuan and Yulin) (In Chinese). The Commercial Press, Shanghai, 128 pp.

Willis, B. and Blackwelder, E., 1907. Research in China (vol. 1). Washington Press of Gibson Brothers, Washington, 516 pp.

Wu, C., Ma, Y., Zhang, X., Wu, J. and Zhao, M., 1999. Topographic surface, Physiographic period and geomorphic evolution of mountain area in the Norht China (in Chinese with English abstract), 286 Heibei Science and Tectnology publishing House, Shijiangzhuang.

Xu, X. and Ma, X., 1992. Geodynamics of the Shanxi Rift system, China. *Tectonophysics*, 208(1-3): 325-340.

Xu, X., Ma, X. and Deng, Q., 1993. Neotectonic activity along the Shanxi rift system, China. *Tectonophysics*, 219(4): 305-325.

Zhang, B., 1959. Mountain geomorphology of Wutai Mountain. *Quaternary Sciences*, 2(1): 39-46.

Zhang, S., Ren, J. and Nie, G., 2007. Paragenesia of Quaternary pediments and river terraces on the north piedmont of Wutai Mountains. *Chinese Science Bulletin*, 52(4): 521-530.

Zhang, Y.Q., Mercier, J.L. and Vergely, P., 1998. Extension in the graben systems around the Ordos (China), and its contribution to the extrusion tectonics of south China with respect to Gobi-Mongolia. *Tectonophysics*, 285(1-2): 41-75.

Zhou, L. and Shackleton, N., 2001. Photon-stimulated luminescence of quartz from loess and effects of sensitivity change on palaeodose determination. *Quaternary Science Reviews*, 20(5): 853-857.

Zhu, R., Laj, C. and Mazaud, A., 1994. The Matuyama-Brunhes and Upper Jaramillo transitions recorded in a loess section at Weinan, north-central China. *Earth and Planetary Science Letters*, 125(1–4): 143-158.

Figures

Fig. 1 General tectonic setting of the Shanxi rift system and its adjacent regions (modified after Zhang et al. (1998)). Inset map showing major faults in China. Abbreviations: DTB, Datong Basin; LFB, Linfen Basin; YCB, Yuncheng Basin; Mt, mountain; R, river. Triangles (reverse faults) and tick marks (normal faults) on hanging wall side.

Fig. 2 (a) Active faults and drainage characteristics of the upper reach of the Hutuo drainage system. The shade relief is from the Shuttle Radar Topographic Mission (SRTM). Small regions in the basin show the sparsely preserved T3. See location in Fig. 1. (b) Isopachs of late Cenozoic sediments in the Xin-Ding Basin modified from Wang et al. (1996). The Xin-Ding basin consists of Daixian, Yuanping, Dingxiang and Dongye subbasins. Towns and villages: LZD, Lingzidi; PS, Pingshang; RJZ, Rongjiazhuang; SHP, Shihouping; ZJZ, Zhaojiazhuang. Active faults: NHF, Northern Hengshan fault; SHF, Southern Hengshan fault; WTF, Wutai fault; XZF, Xizhou fault; YZF, Yunzhong fault. R, river; Mt, mountain.

Fig. 3 Correlation of loess stratigraphy in the Chinese Loess Plateau and the Marine istoope curve. Chinese loess sequence is from the Jingbian section in northern China (Ding et al., 2005); the $\delta^{18}O$ records from Lisiecki and Raymo (2005); the B/M (Brunhes/Matuyama) boundary after Zhu et al. (1994).

Fig. 4 Longitude profile in the upper reach of the Hutuo River. Vertical bands represent river terraces,

and their heights are from field measurements. Riverbed and topography of the drainage divide are derived from the 25-m-resolution digital elevation model data. Paleolake level is estimated from field observations (see text for details).

Fig. 5 Cross section of fluvial terraces of the Hutuo River in the Xin-Ding basin along a-a'. See location in Fig. 2a.

Fig. 6 Photo (a) and characteristics of terrace fill (b) of T3 west of Sulongkou Village (N38º56'34.6", E112º50'13.7"). See Fig. 2a and 4 for location.

Fig. 7 Terrace sequence around Jiehepu. See location in Fig. 2a. (a) Cross section of fluvial terraces. (b) Terrace fills of T3 and T1 at Jiehupu (N38º37'53.4", E112º43'44.5"). (c) Magnetic susceptibility curve of loess on T2. (d) Terrace fill of T3 west of Jiehepu (N38º38'14.4", E112º42'56.8"), and its overlying loess-paleosol section determined by magnetic susceptibility measurement (e). Above S1, there is a loess unit (L_1) with an interbedded gray fine sand layer, which might result from a large flood during the formation of L1. R, river; V, village.

Fig. 8 Terrace sequence of the Hutuo River at Rongjiazhuang Village (N38º29'54.5", E113º13'38.2"). (a) Distribution map of river terraces. Contour lines (10 m interval) are from the topographic map (1:10,000). The projection coordinate system is WGS84-UTM. See location in Fig. 2a. (b) Terrace fill of T3 and the overlying loess-paleosol section. (c) Cross section of fluvial terraces of Hutuo River. See profile location in Fig. 8a.

Fig. 9 Terrace sequence of the Hutuo River at Zhaojiazhuang Village (N38º28’12.0”, E113º13’56.9”). (a) Distribution map of river terraces. Contour lines (10 m interval) are from the topographic map (1:10000). See location in Fig. 2a. (b) Cross section of fluvial terraces. See location in Fig. 9a. (c) Terrace fill of T3 and the overlying loess-paleosol section.

Fig. 10 Terrace sequence of the Hutuo River at Lingzidi Village (N38º26’33.3”, E113º14’07.0”). (a) Distribution map of terrace sequence based on field investigations and the interpretation of high-resolution satellite images. Contour lines (10 m interval) are from the topographic map (1:10000). See Fig. 2a for location. (b) The overlying paleosol (S_1) on T3, north of Lingzidi Village. (c) Photo showing the terrace sequence from T3 to T1, north of Lingzidi. See location in Fig. 10a. (d) Magnetic susceptibility curve of loess on T2. (e) Cross-section profile of the Hutuo River at Lingzidi Village. See location in Fig. 10a. AR, Archean.

Fig. 11 (a) Geological map of the Shihouping-Pingshang transverse drainage across the Xin-Ding basin and Hutuo drainage to the north and south. See location in Fig. 2a. Inset rose diagrams of clast dip direction data for discoidal clasts in terrace gravel. Lithological data are compiled from the geological map (1:200,000): Q, Quaternary fluvial gravel and loess; C-P, Carboniferous-Permian limestone; ∈-O, Cambrian-Ordovician limestone with siltstone; Ar, Archean metamorphic rocks; Pt, Proterozoic metamorphic rocks. (b) Oblique Google image showing geomorphology at the Shihouping-Pingshang transverse reach.

Fig. 12 Cross section of terrace sequence of the Qingshui River at Hujiazhuang Village (N38º32’58.9”, E113º21’51.1”). See Fig. 11a for location.

Fig. 13 Drilling profile of the Dongye subbasin (No. 601 Geological Team of Geological Bureau of Shanxi Province, 1960). See location in Fig. 11a.

Fig. 14 Lacustrine deposits (a) under fluvial sand of T3 and cross section of terraces (b) of the Hutuo River at Tanglingang Village (N38º39’43.3”, E112º43’54.3”). See location in Fig. 2a and 4.

Fig. 15 (a) Paleolake deposits and the overlying loess in the Dongye Basin (N38º36’19.9”, E113º09’19.1”). (b) Cemented gravels west of Liujiazhuang Village (N38º34’48.1”, E113º13’38.6”), indicating a northeast-flowing direction as rose diagram of clast imbrication in Fig. 11a. See their locations in Fig. 11a.

Fig. 16 Paleogeographic reconstructions for each of the stages of drainage development: (a) the Piocene, (b) Early-Middle Pleistocene and (c) since Late Pleistocene. See text for details. Maps compiled from data presented within this paper together with the studies of Willis and Blackwelder (1907), Li and Liang (1965), Wang et al. (1996) and Li et al. (1998). Background is the SRTM digital elevation model data. Thick blue lines represent main streams and thin lines indicate tributaries. White arrows represent flow directions. The extent of the Xin-Ding paleolake is shown by solid region in Fig. 16b, estimated by field survey at natural outcrops. Abbreviations: DC, Doucun; DX, Daixian; DXC, Dingxiang County; DY, Dongye; TLG, Tanglingang; XZ, Xinzhou; YP, Yuanping County; WT, Wutai

County.

Figure1
Click here to download high resolution image

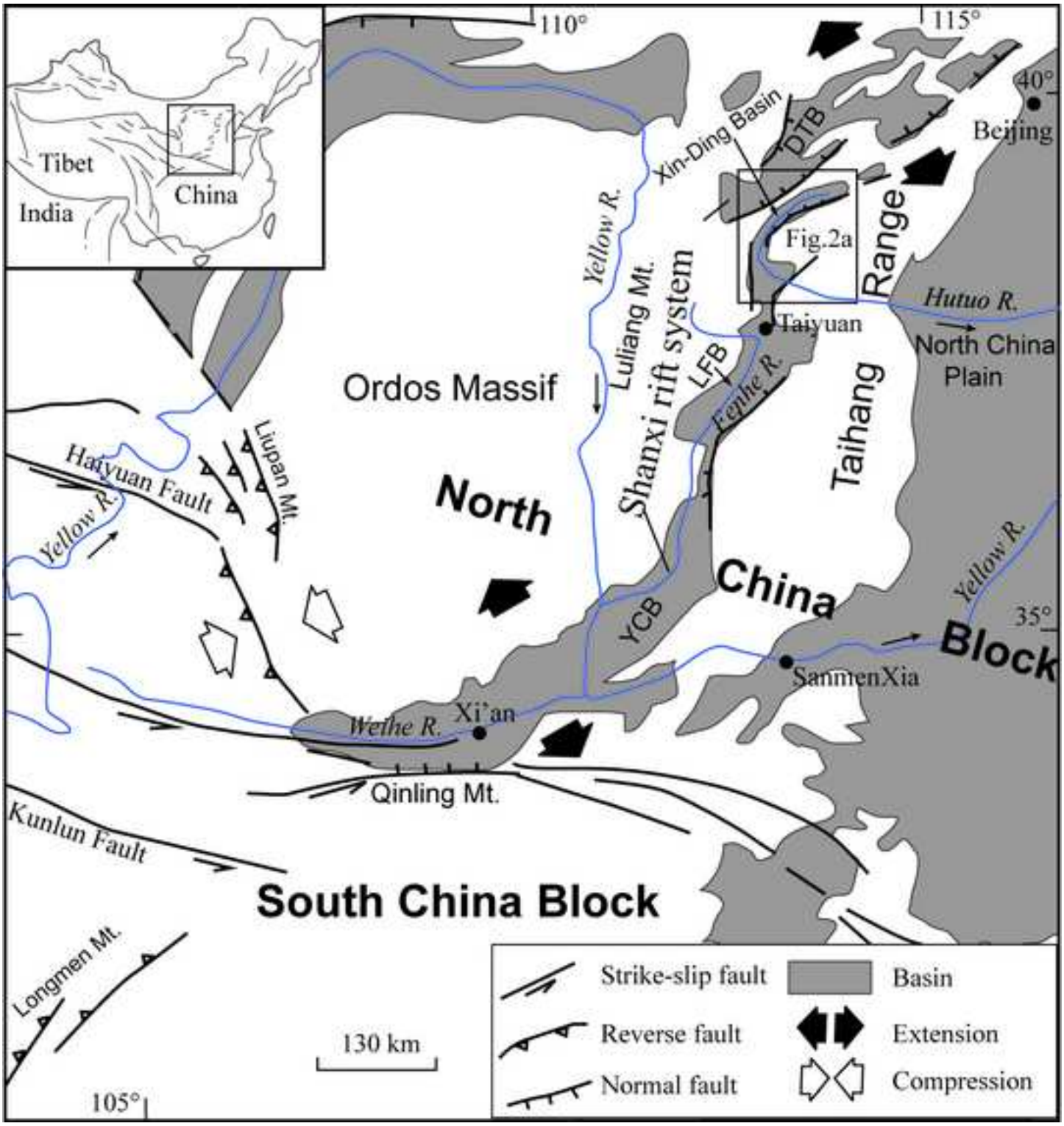

Figure2

Click here to download high resolution image

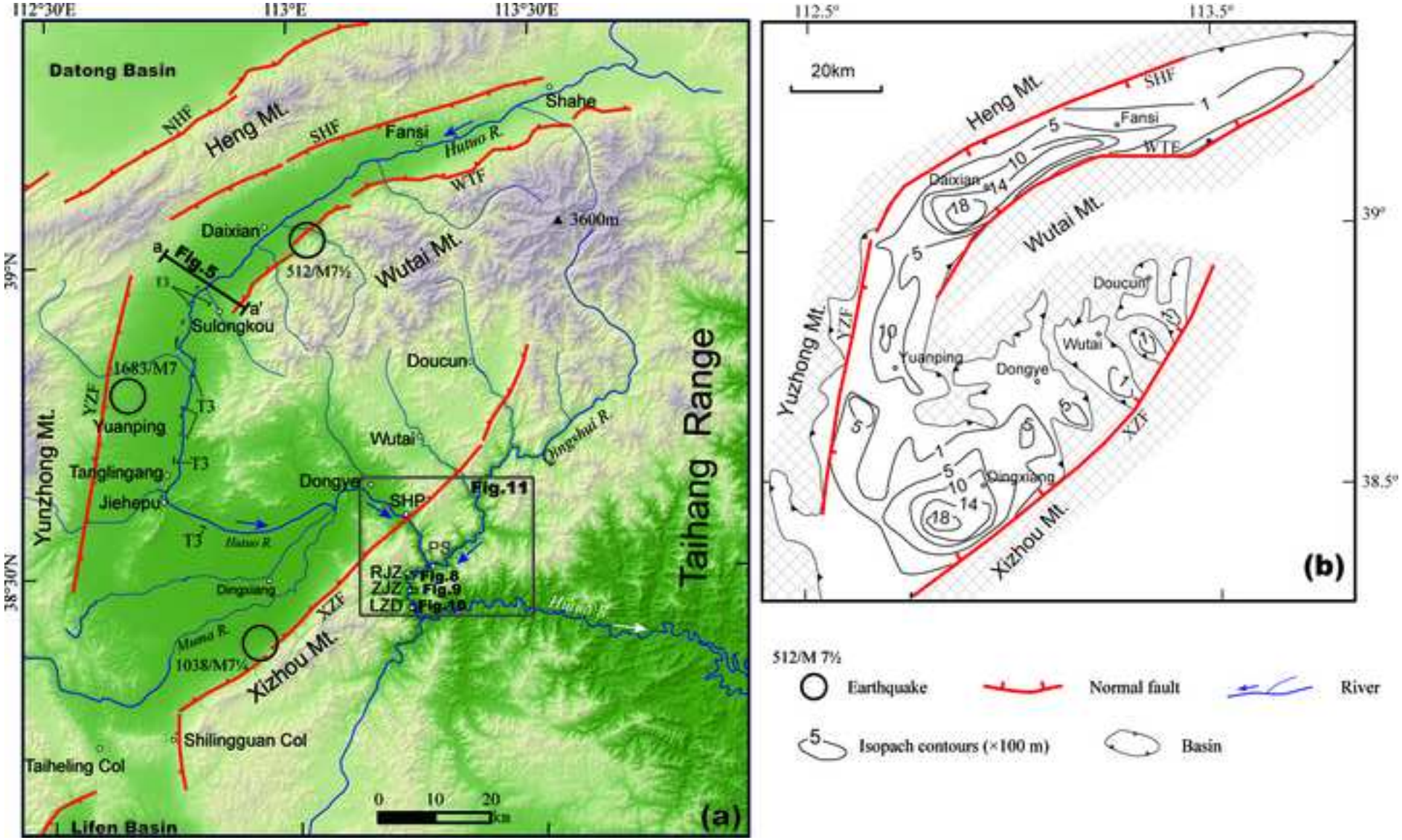

Figure3
Click here to download high resolution image

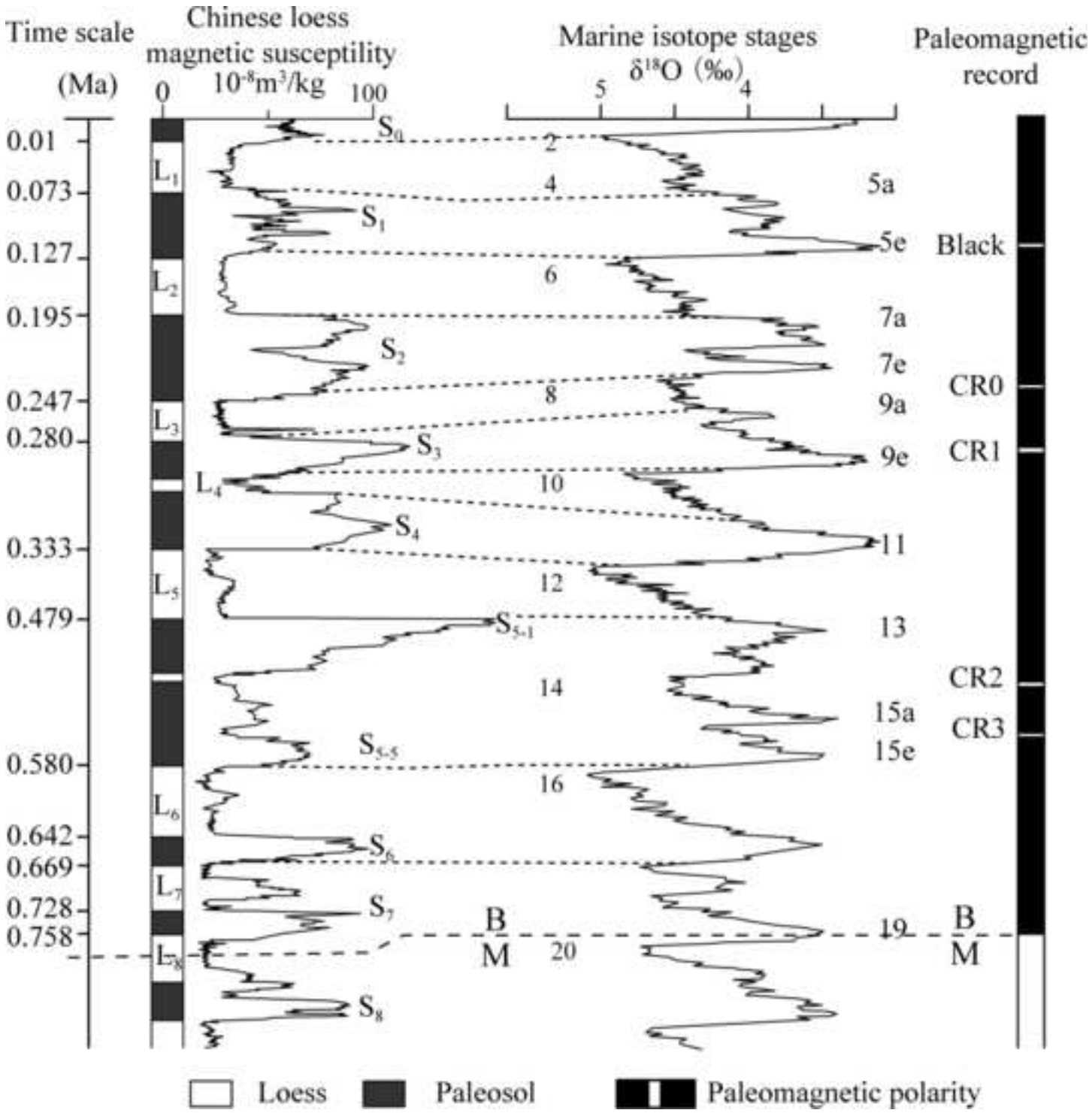

Figure4
Click here to download high resolution image

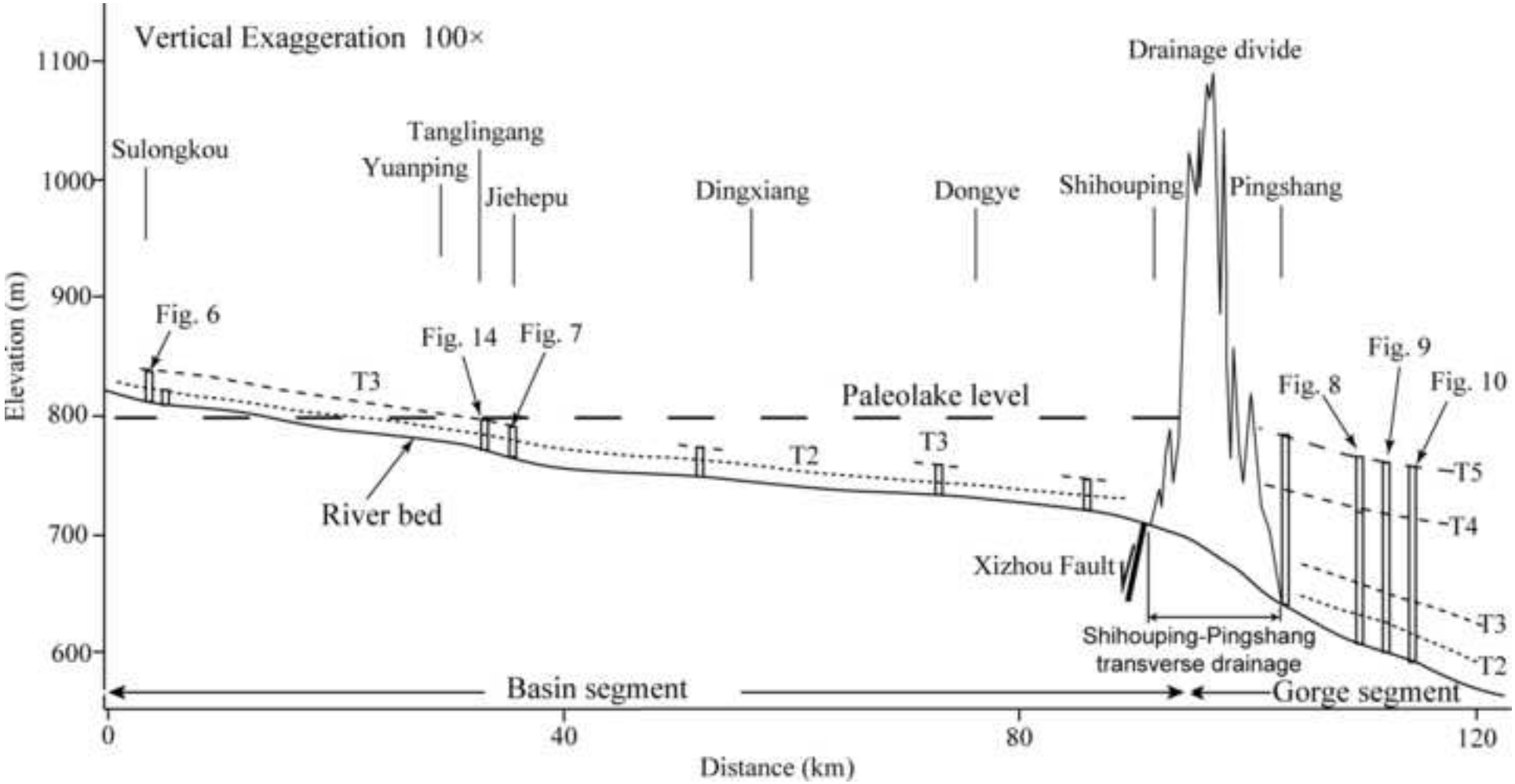

Figure5
Click here to download high resolution image

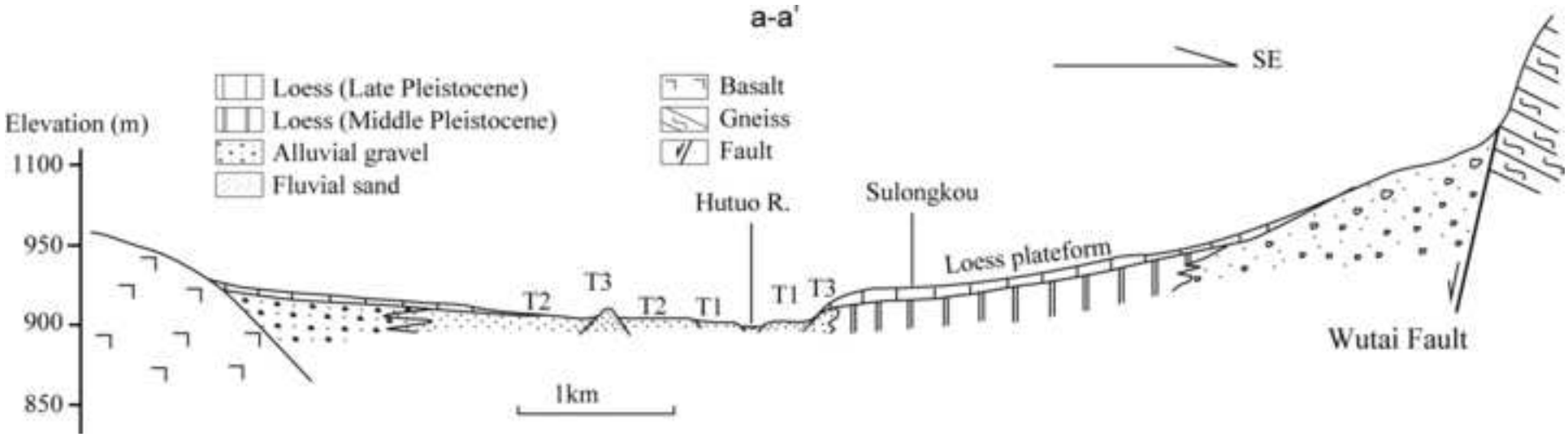

Figure6
Click here to download high resolution image

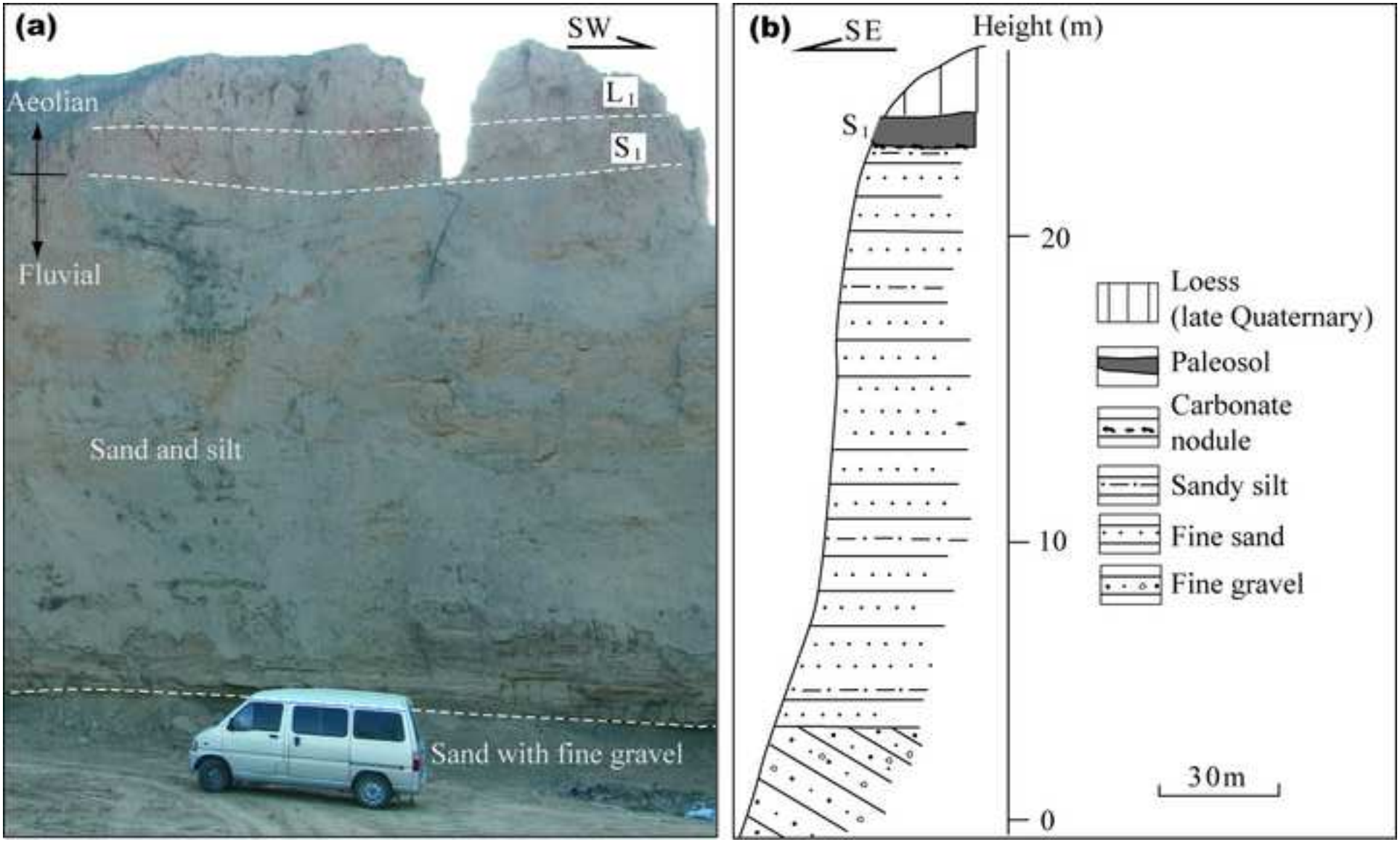

Figure7
Click here to download high resolution image

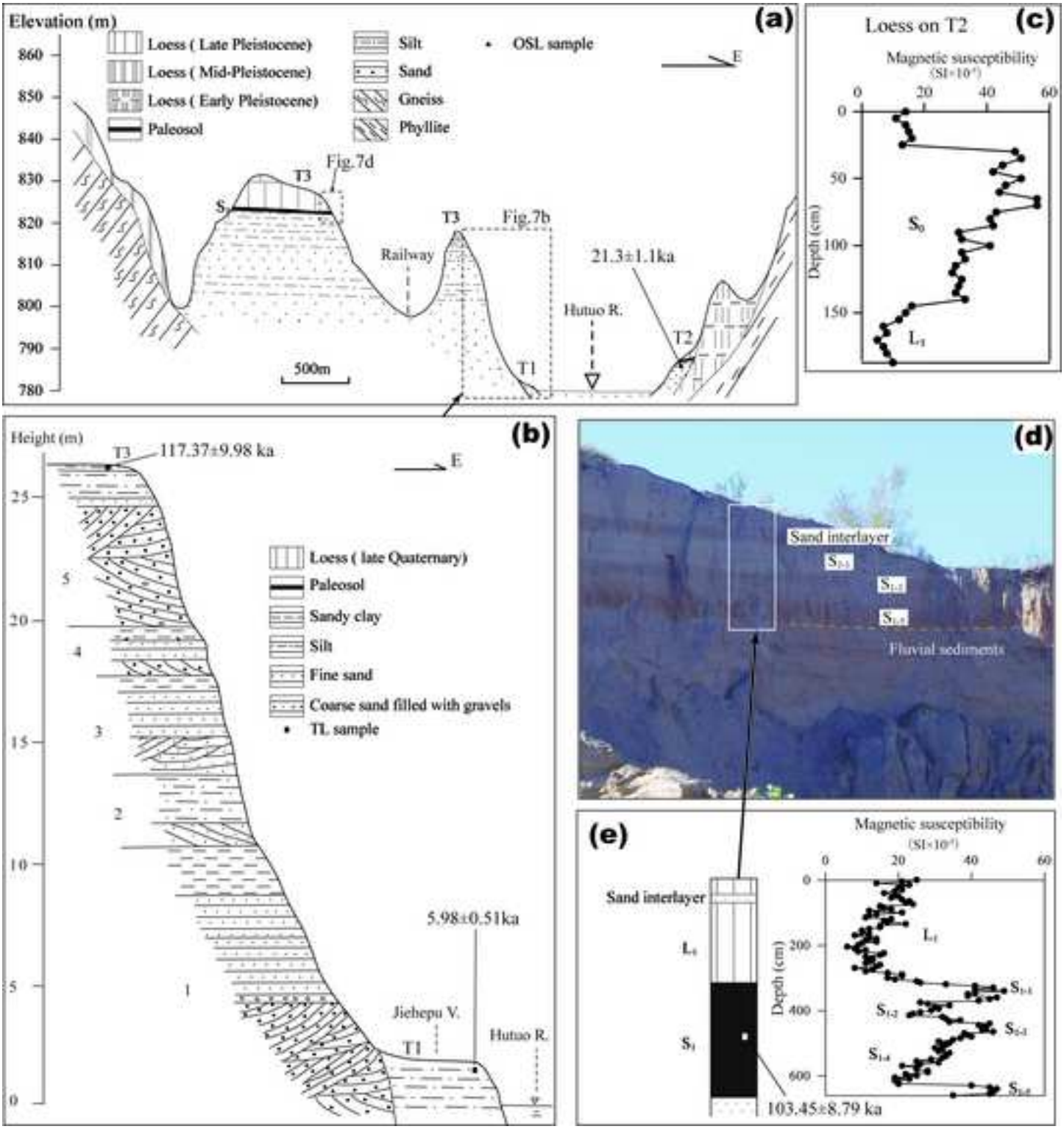

Figure8
Click here to download high resolution image

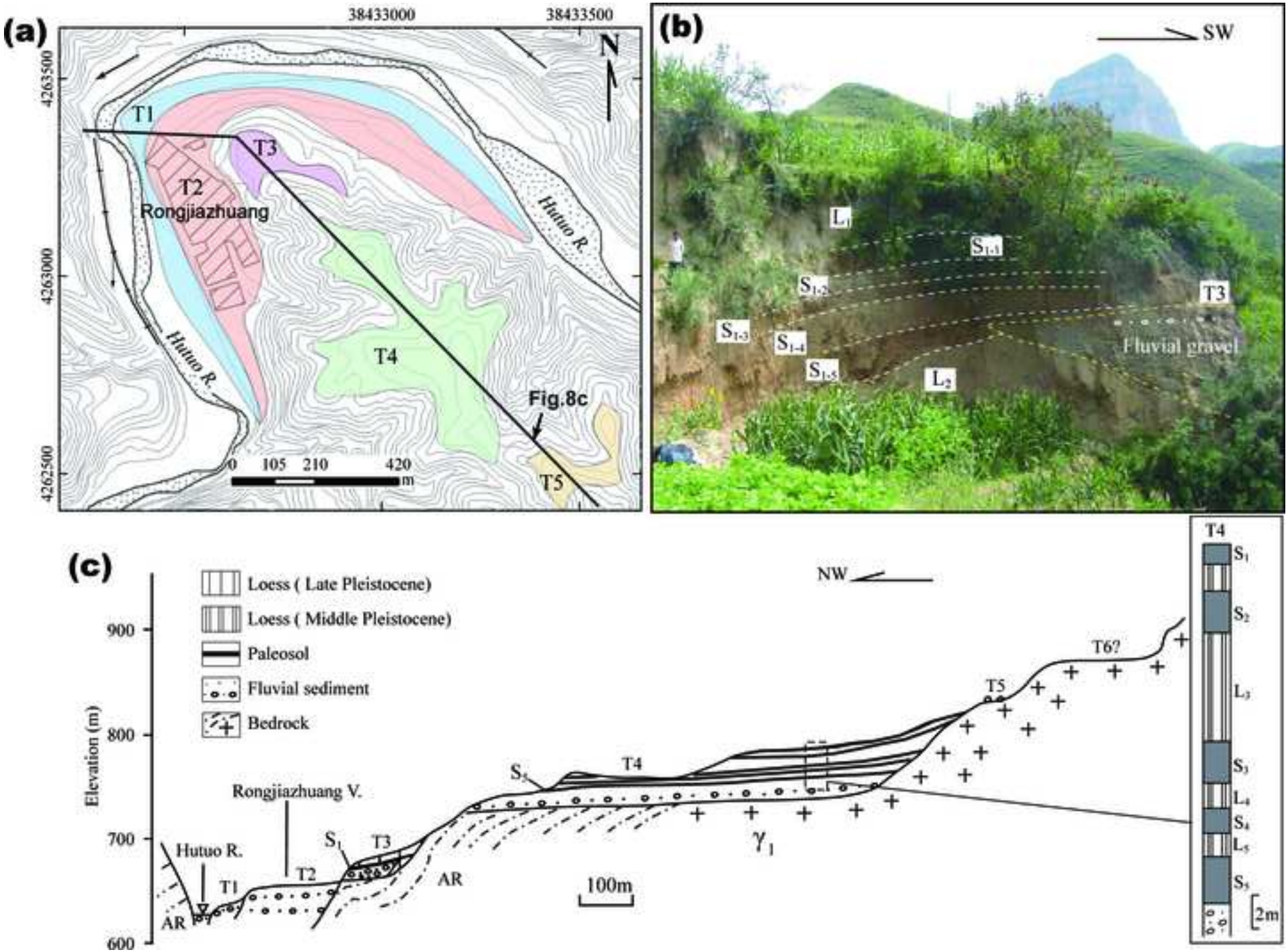

Figure9
Click here to download high resolution image

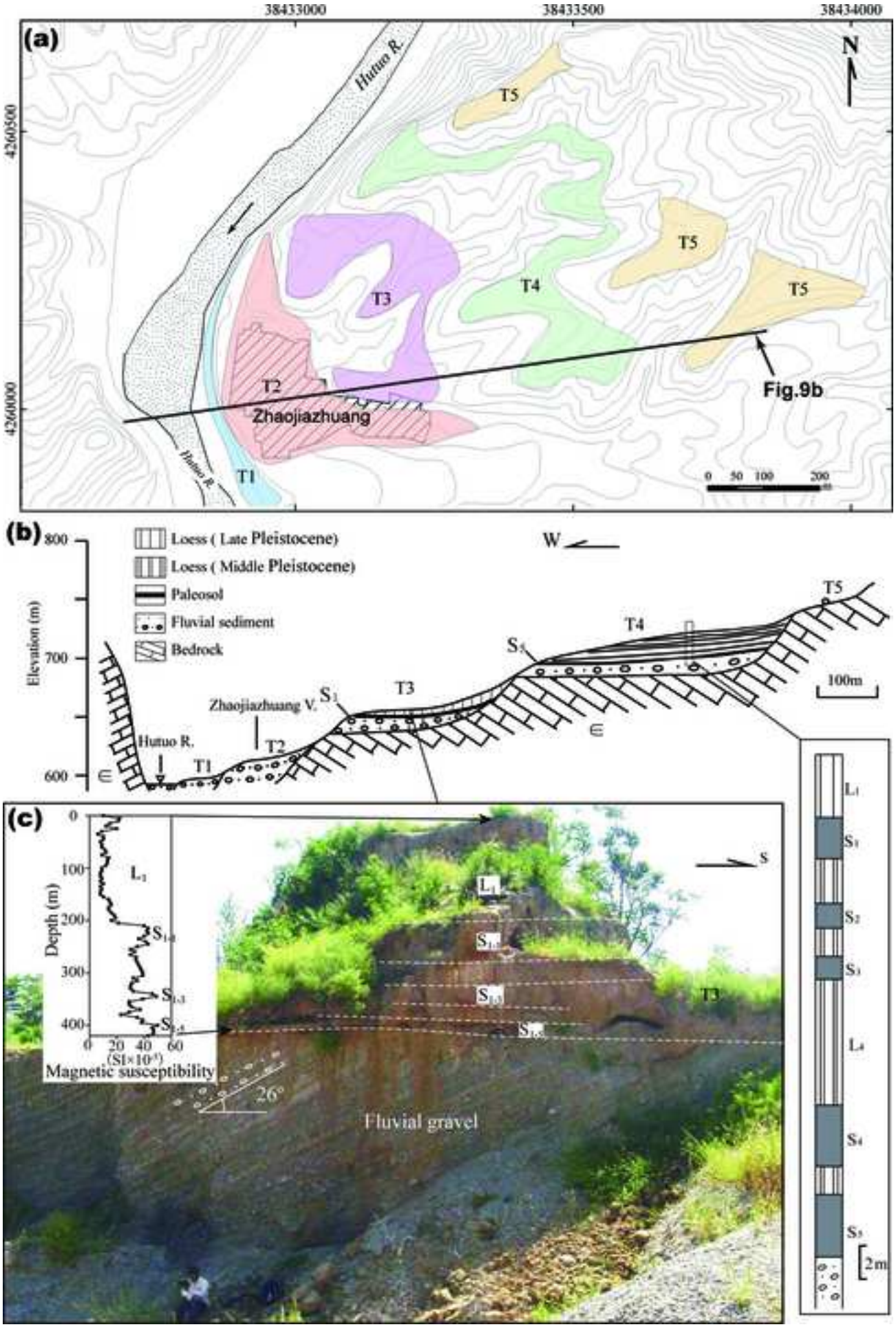

Figure10
Click here to download high resolution image

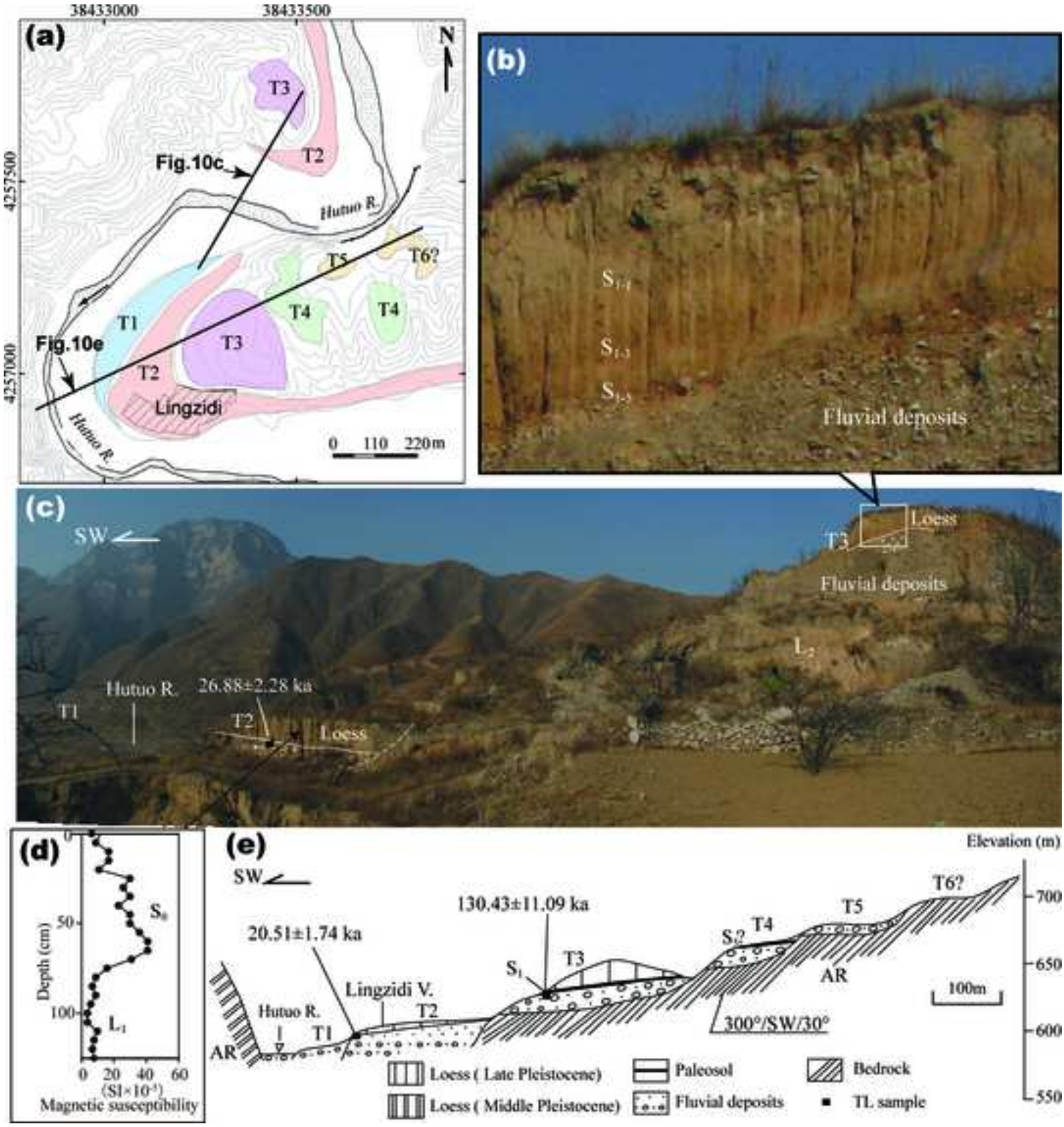

Figure11
Click here to download high resolution image

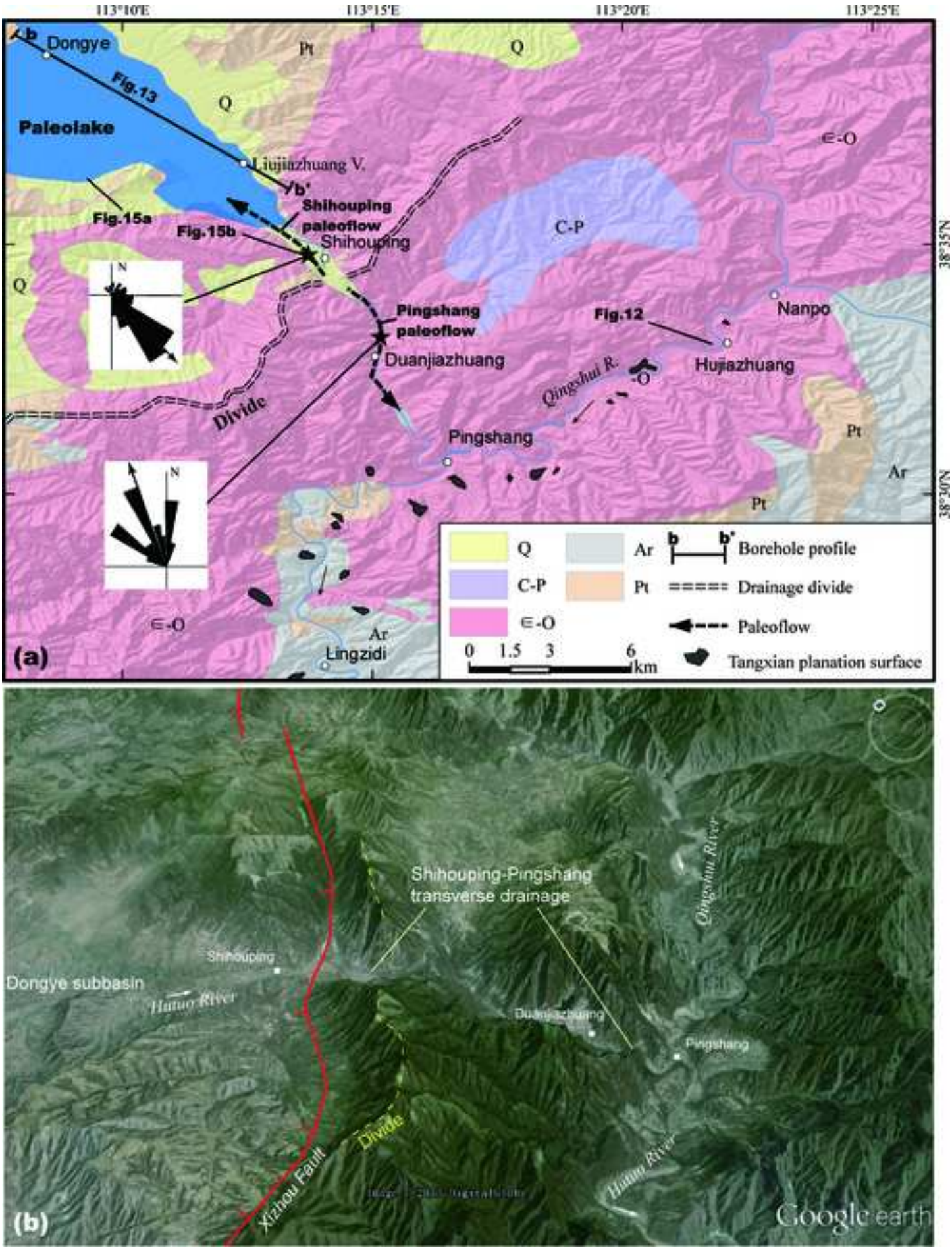

Figure12
Click here to download high resolution image

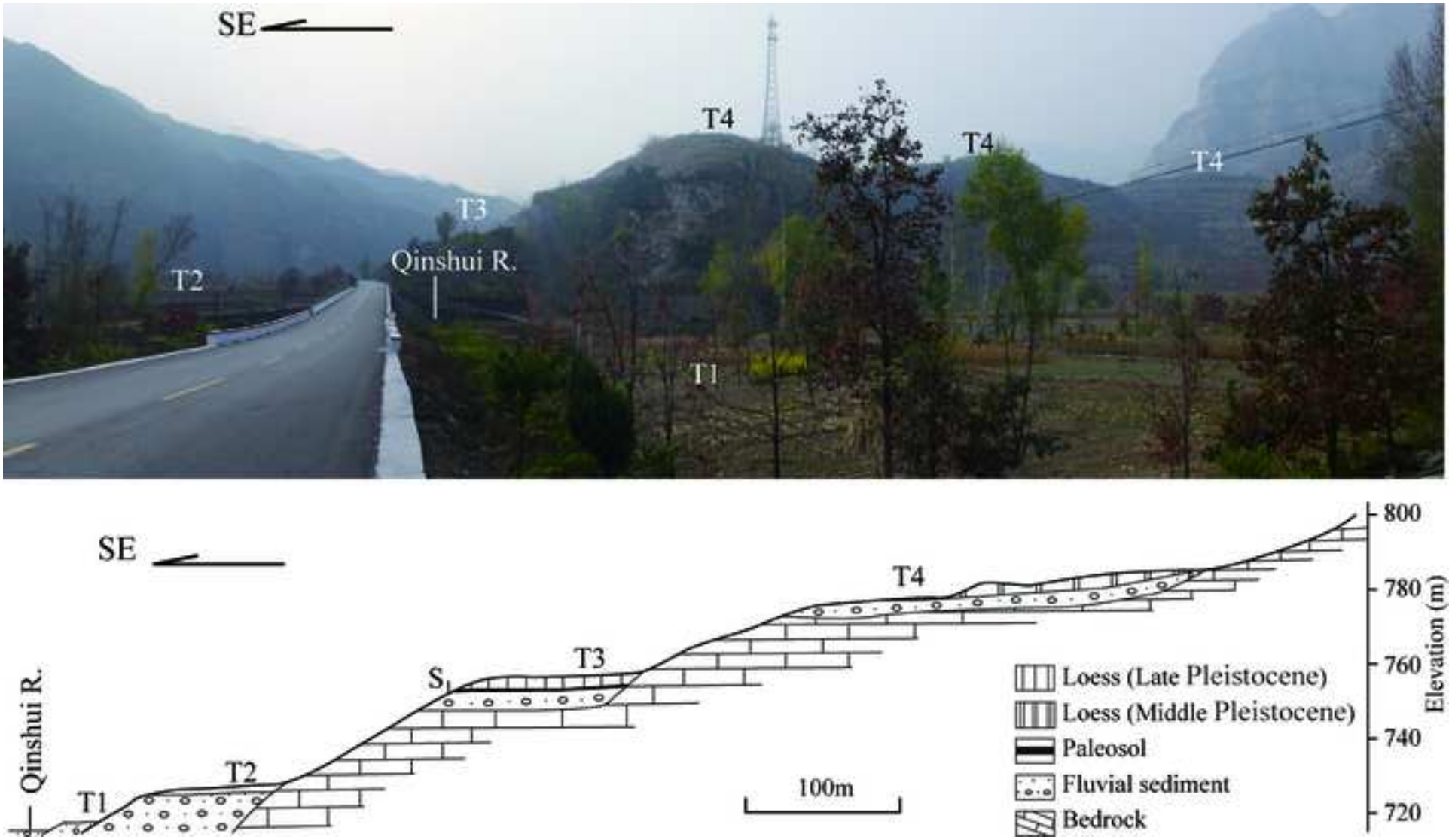

Figure13
Click here to download high resolution image

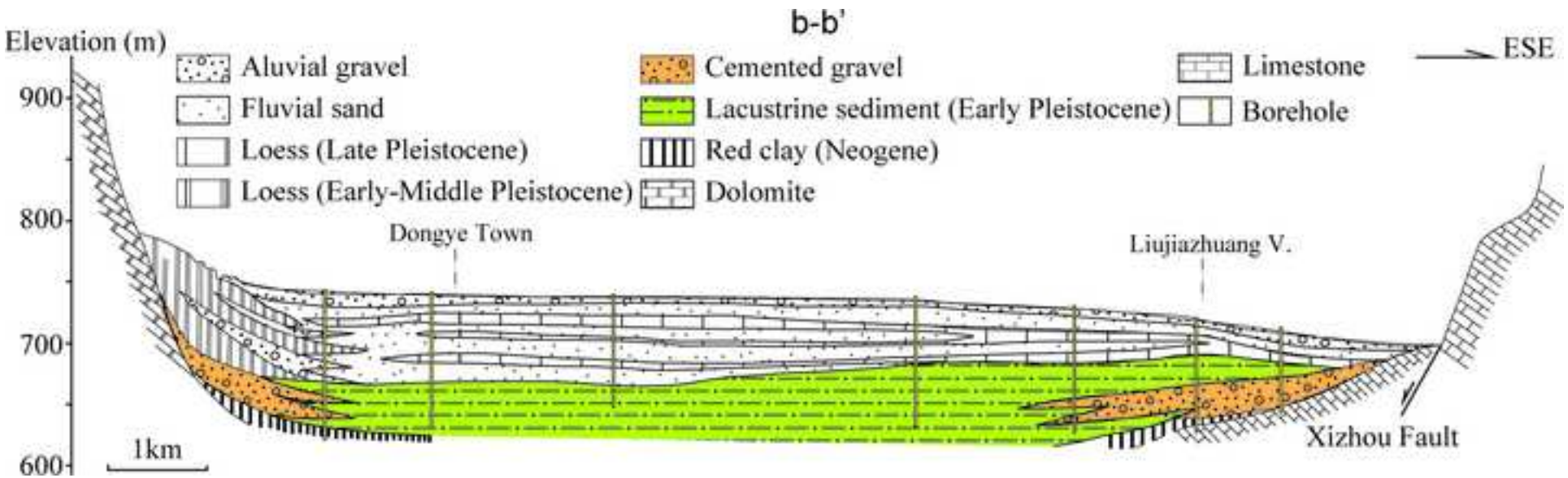

Figure14
Click here to download high resolution image

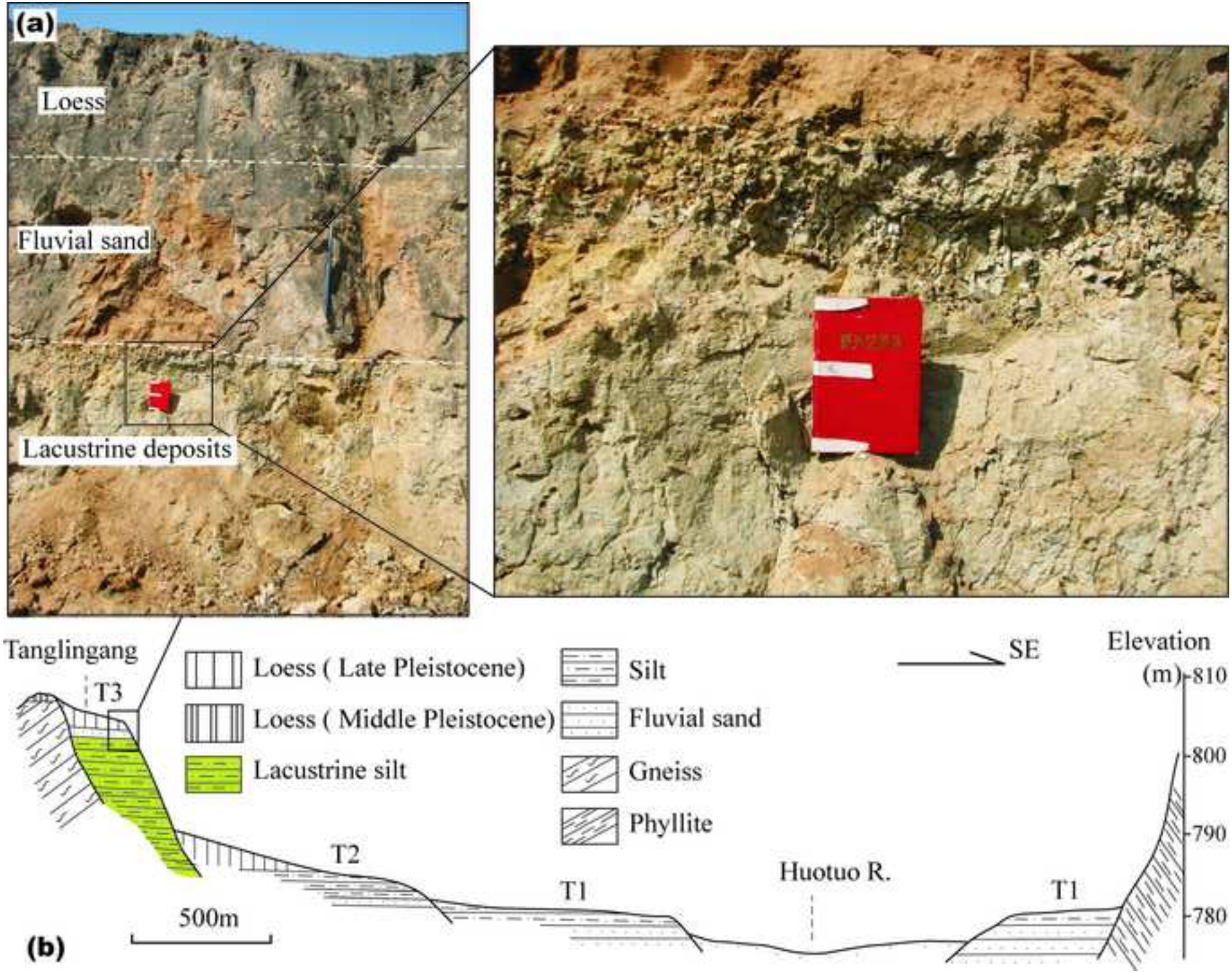

Figure15
Click here to download high resolution image

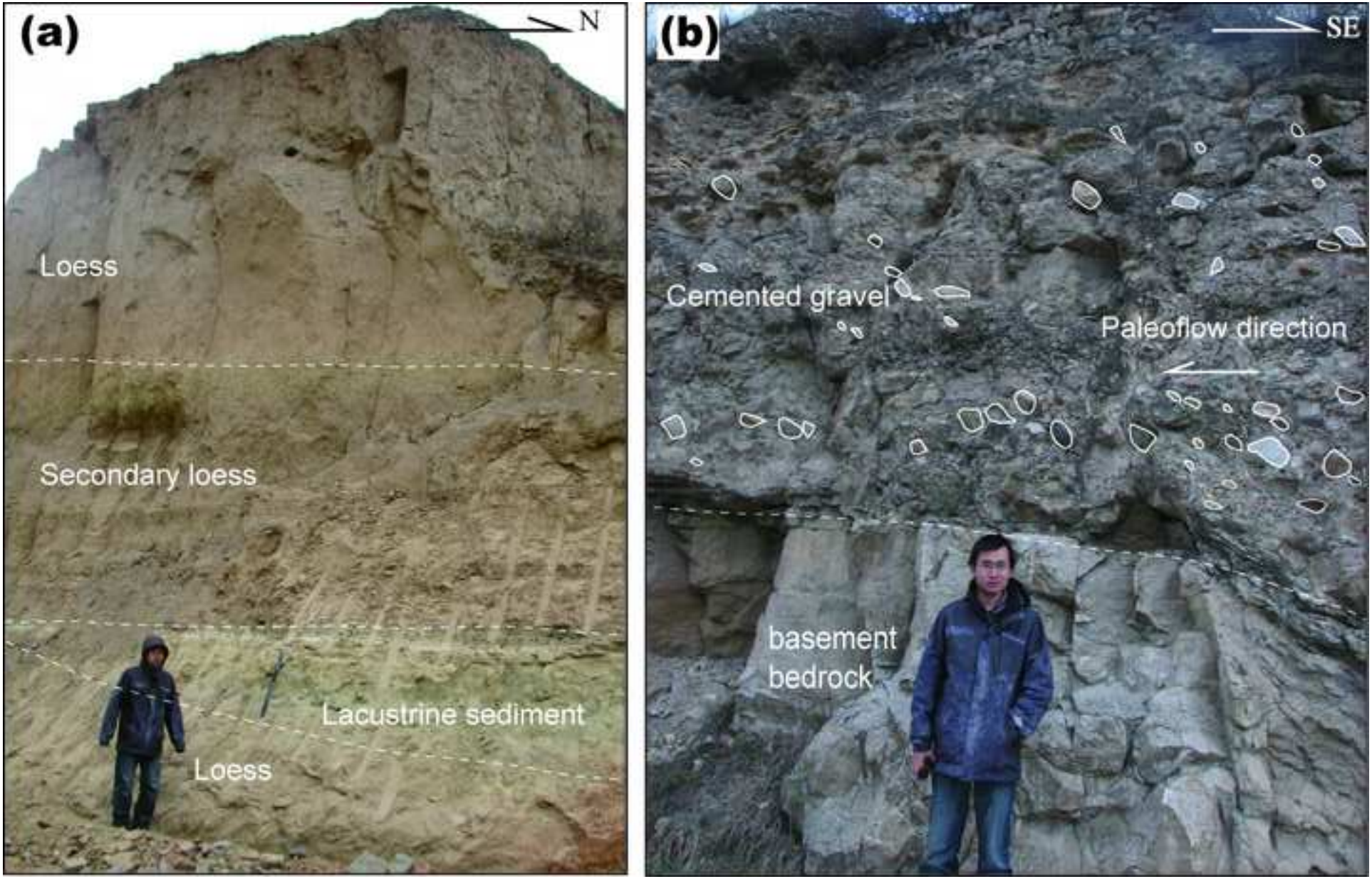

Figure16

Click here to download high resolution image